SLOVAK UNIVERSITY
OF TECHNOLOGY IN BRATISLAVA
FACULTY OF ELECTRICAL ENGINEERING
AND INFORMATION TECHNOLOGY

Ing. Stanislav Pecko

Summary of doctoral dissertation

ANALYSIS OF REACTOR PRESSURE VESSEL STEELS USING POSITRON ANNIHILATION SPECTROSCOPY

for the acquisition of: academic title philosophiae doctor, PhD.

in doctoral study programme: **Nuclear Power Engineering**

and study field: 5.2.31 Nuclear Power Engineering

Date and place: In Bratislava, January 2017

ABSTRACT

A research of radiation damage in western reactor pressure vessel (RPV) steels using mainly positron annihilation spectroscopy (PAS) is a major goal of this dissertation thesis. This non-destructive experimental technique can offer a unique view of materials microstructure from a quantitative and qualitative analysis of vacancy-type defects point of view. A sensitivity of PALS is relatively very high with an ability to recognize one defect per 10^7 atoms in crystal lattice. The research is focused on commercial Germen RPV steels P370WM and P16WM and Japan model RPV steel JRQ and JPA. The steels were irradiated by neutrons or light (H^+) and heavy (Fe^{2+}) ions in different fluencies, or in addition JRQ steel was thermally annealed. Specimens were experimentally measured by different PAS techniques – positron lifetime measurement, conventional or slow-positron Doppler broadening in order to get a depth profile of defects. PAS experiments were analysed and compared with other experimental techniques, such as nanohardness, Vickers hardness or small-angle neutron scattering (SANS). Results are analysed and compared in terms of size and concentration of defects and the influence of chemical composition (mainly influence of Cu) of the studied steels to radiation damage evolution of different types and fluencies of irradiation. A comprehensive analysis of the effects of radiation damage, in terms of defects in the microstructure, hardness and possibility to simulate neutron irradiation by implantation of light and heavy ions into RPV steels, was created as the output of this dissertation thesis.

CONTENTS

1 INTRODUCTION

A lot of currently operated nuclear power plants (NPP) have reached or will reach their projected lifetime in the following years. Nowadays, a mean age of operated NPPs is around 30 years, which brings us to a very current issue of NPPs lifetime prolongation. These procedures contain a lot of features, such as licensing and an assessment of technical conditions of different parts of NPP. From technical point of view, reactor components must be able to withstand a long-term safe operation in perfect condition for another 10-30 years. Ageing is connected mainly with mechanical and material degradations and many of the components can be easily replaceable if it will be necessary.

In this thesis I aim at investigation of radiation effects on Reactor Pressure Vessel (RPV) steels. RPV is a crucial irreplaceable component of nuclear power plant (NPP) and must be capable to withstand the whole set of effects of a reactor environment. RPV determines an overall lifetime of the nuclear facility, because it is not generally feasible to replace RPV. Experimental investigations of various neutron and ion irradiated RPV steels were based mainly on different Positron Annihilation Spectroscopy (PAS) techniques complemented by hardness measurements and compared with other different experimental methods. As a result, this thesis brings a quite unique comparison between neutron and Fe^{2+} and H^{+} ion irradiation performed on such complex materials as RPV steels are.

2 AIMS OF THE THESIS

This dissertation thesis is focused on these scientific items:

1. Consideration of NPPs operation beyond the period of projected lifetime influence the condition of RPV steels in terms of a long-term sustainability of the reactor vessel.

2. Analysis of the most influencing features to irradiation embrittlement in medium-Cu RPV steels with the focus on vacancy-type defects and evaluation of its influence to radiation hardening.

3. Evaluation of the options of neutron irradiation simulation via ion irradiation. Evaluation of the differences between heavy and light ion irradiation in such complex materials as RPV steels.

4. Application of PAS techniques and evaluation of their suitability and contribution for studying of irradiated RPV steels for overall understanding of irradiation features and defects identification.

5. Evaluation of the influence of different Cu contents in RPV steels by means of PAS focused on Cu precipitation during neutron and ion irradiation.

3 STATE OF THE ART

The radiation damage on reactor steels is caused by neutron irradiation mainly. Other radiation (alpha, beta and gamma) cause damage on an insignificant level compared to neutrons. Neutrons can knock-out an atom from the crystal lattice (make cascade formations – caused by fast neutrons) or cause transmutation of one element to the other one (usually radioactive – caused by thermal neutrons), what results to change of the nuclear, physical, mechanical and chemical properties of the material.

There is always some number of defects presented in crystal lattice of metal materials; even defects are formed during a manufacturing process. These defects, most of vacancy type, can change over time, recombine or accumulate to formations by the influence of irradiation, temperature or chemical effects. The point defects are especially dangerous in BCC structures, where they are responsible for a smaller ductility of the material, decrease of offset yield strength and total embrittlement. Elements of light gases, such as helium and hydrogen, can be created by fast neutrons during nuclear reactions {(n-p) and (n-α)}. These gas atoms can merge into gas bubbles, which grow and can create voids. This results to the material growth, where tension and brittleness are increased.

The most important factors of the degradation of RPV steels are neutron fluence (creating of the defects) and temperature (annealing of the defects). The microstructural changes of the structure materials result from a mutual balance between the radiation damage and the thermal annealing. The main degradation processes include radiation hardening, embrittlement, swelling, corrosion and ageing. The degradation of RPVs connecting all these aspects leads to an overall change of various interconnected material properties. A change of one of the aspects can lead to a change of another aspect in both ways, positively or negatively. There is often a hard task to find the best optimal conditions in order to minimalize impacts of irradiations or other influences in nuclear reactors.

Radiation embrittlement is caused mainly due to irradiation temperature, neutron fluence, and neutron flux factors, and depends strongly on the chemical composition of the irradiated material. RPVs are irradiated at temperature about 300 °C and it is believed that embrittlement is the result of irradiation-induced fine-scale microstructural features of defects. These features act as obstacles to a free movement of dislocations, what generates an increase of yield strength (hardening) and move the transition temperature to lower values (embrittlement). Theoretical and experimental observations suggest that these defects are mainly of two types [1]:

- **Radiation damage clusters** – vacancy clusters or microvoids created by neutron-lattice atomic interactions (matrix displacement damage).
- **Metallic clusters** – solute clusters formed during the irradiation due to enhanced solute diffusivity resulting from the elevated point defect population.

About 70-80% of an embrittlement effect is attributed to the metallic clusters. The biggest influence on radiation embrittlement has Cu and P and less other precipitates. The annealing experiments indicate that microvoids and vacancy clusters are responsible for 20-30% of RPV steels embrittlement. However, these defects were detected only in model irradiated steels; in the commercial RPV steels is no reliable evidence of their incidence [1]. In the picture (Fig. 3.1) is illustrated a proportion of each effect to whole embrittlement of RPV steels as the neutron fluence dependence [2].

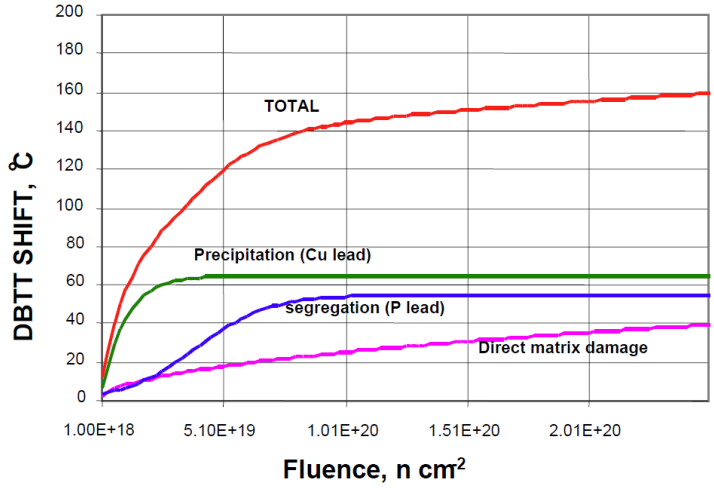

Fig. 3.1 - Scheme of irradiation embrittlement mechanisms calculated by a semi-mechanistic analytical model [2]

There is a general consensus of the embrittlement mechanism [3]. Cu atoms precipitate and make formations of Cu-enriched clusters (diameter of 2-3 nm) and then behave like obstacles and hinder dislocation movements. Cu core is associated with other elements; such as Ni, Mn, Cr, P and Si, which follow and bind together with Cu precipitates. P segregation weakens grain boundaries. On the other side, the formation of matrix damage, such as point defect clusters (dislocation loops or vacancy clusters) is a main contributor to embrittlement of low Cu materials. Ni has a synergetic effect with Cu, but it causes hardening even in very low or no Cu materials. Effect of P plays a role in low Cu materials but in high Cu materials is not evident.

Experimental irradiation of materials can be done by various approaches. The best option is irradiation in nuclear reactors, either by commercial NPP as a part of surveillance programmes or in material test reactors (MTR). These options are ideal from simulation of real neutron damage aspects, where the same features are reached as in commercial reactors. But, there are a lot of disadvantages – radioactivity of the material, which complicate rapidly a handling, transportation, storage, polishing and measurements. Also, a new radioactive waste is always made after neutron irradiation and moreover, costs are always much higher by irradiation in reactors and the time of irradiation is very long (~1 year in commercial reactors) [4].

Although, the neutron irradiation cannot be replaced by anything due to its neutral charge resulting to extraordinary features and with a characteristic behaviour of the interaction with the matter, there is used various different approaches to experimentally simulate the neutron damage. A basis of the neutron simulation methods is built on an acceleration of electrons and ions of different types and energies. Basically, there are different approaches of ion irradiation – by light ions (H, He) and by heavy ions (Fe), or there should be combinations of them. Especially, light ions can simulate primary knocked atoms and heavy ions secondary collisions. Triple beam (Fe+He+H) is considered as the state-of-the-art of ion irradiation worldwide, where advantages of each ion types contribute to a whole irradiation profile. The question of possibility to use ion irradiation to irradiation of commercial RPV steels is still under discussion due to a very complex origin of such steels. Ion irradiation can be an option, where the surveillance material is simply consumed or there are available only small amounts of unirradiated archive material or reminders of tested surveillance samples, within reasonable time. Another issue is that a damage layer has a steep damage distribution and the damage is only in the thin surface layer [5].

4 MATERIALS CHARACTERIZATION

4.1 German RPV steels

All specimens (two pieces from each set to covering the positron source) were delivered from AREVA NP GmbH Erlangen and belong to commercial RPV steels used since 70-ties in Germany. These steels have been comprehensively studied in the research projects CARISMA [6] and CARINA [7]. Materials are from weld material (marked as WM) of the RPV. As-received (unirradiated) specimens, in the form of slides with dimensions of 10x10x0.2 mm, were polished to shape "like mirror" by a 1 μm diamond paste. The irradiation was performed in the VAK reactor, whereat the irradiation temperature was mainly in a range between 280 - 290°C. Irradiated specimens, in the form of slides with dimensions of 10x10x1 mm, were also prepared for the measurements, but just by cleaning in an ultrasonic bath. The chemical composition of the studied German steels is listed in Tab 4.1.

Tab. 4.1 – Chemical composition of studied German RPV steels from CARINA-CARISMA projects in wt% (balance to Fe)

Steel	C	Si	Mn	P	S	Cr	Mo	Ni	Cu
P370 WM	0.08	0.15	1.14	0.015	0.013	0.74	0.60	1.11	0.22
P16 WM	0.05	0.15	1.14	0.012	0.007	0.07	0.46	1.69	0.08

There were two irradiated materials P16WM and P370WM and each of them has two different cuts from the same bulk. In Tab. 4.2 are shown neutron fluence and an activity of the measured specimens. Irradiated samples are also specific from the chemical composition point of view. The P370WM is a material with the highest content of Copper (0.22 wt%) and P16WM is a material with the highest content of Nickel (1.69 wt%) in the CARINA-CARISMA projects. These limit contents of Cu and Ni should strongly affect the final radiation damage due to a negative impact of these impurities on radiation and mechanical properties. The P370 WM specimen was also used in unirradiated condition to a hydrogen ion implantation in order to perform a simulation of neutron irradiation and make possible to compare both: neutron and ion irradiation, from the defect size and concentration point of view.

Tab. 4.2 – Neutron fluence and measured activity on 24 January 2013

Specimen	P370WM-D77	P370WM-D161	P16WM-S103	P16WM-GS67
Fluence [cm^{-2}]	$2.21x10^{19}$	$2.23x10^{19}$	$1.16x10^{19}$	$4.81x10^{19}$
Activity [kBq]	12.85	97.31	40.09	16.6

4.2 Japan model RPV steels

Specimens from JRQ and JPA family of RPV steels correspond to the specification of ASTM A533B cl.1 steels [8]. They were manufactured by Kawasaki Steel Corporation in Japan according to the order of the International Atomic Energy Agency (IAEA) and were used in various studies focused mainly on neutron embrittlement of various levels of irradiation and annealing conditions since 1980s. The goal was to obtain a comprehensive database of mechanical and physical measurement data for a better understanding of the mechanism of neutron embrittlement and the subsequent possibility for evaluation of annealing procedure in order to improving the mechanical behaviour of materials. The chemical composition of the studied steels is given in Tab. 4.3. The main difference of these steels is in Cu content, which is in both cases higher as actual recommended level 0.008% [1, 8].

Tab. 4.3 – Composition of the materials in wt% (balance to Fe)

Steel	C	Mn	Si	Cr	Ni	Mo	V	S	P	Cu
JRQ	0.20	1.42	0.23	0.13	0.80	0.52	0.008	0.005	0.02	0.15
JPA	0.18	1.33	0.26	0.16	0.73	0.55	0.006	0.004	0.02	0.29

JRQ steel was produced by the Basic oxygen furnace-ladle refining furnace (BOF-LRF) process. After rolling, plates (225 mm thickness) were heat treated under the following conditions: normalized at 900 °C, quenched at 880 °C, tempered at 665 °C for 12 hours and stressed relieved at 620 °C for 40 hours [9]. JRQ was proposed as a correlation monitor, which means a material with medium sensitivity to radiation damage (simulation of RPVs steels of older NPPs). JPA steel, designed as special model alloy (Cu content of 0.29 wt% was chosen to represent steels with increased Cu content for a research conducted on high-Cu RPV steels), was produced by the same process of BOF-LRF. After rolling, plates (30 mm thickness) were heat treated under the following conditions: normalized at 900 °C, quenched at 880 °C, tempered at 670 °C for 80 minutes [10].

Our specimens were delivered from HZDR, where were used for many SANS and hardness experiments and results were published in [10, 11]. Also mechanical properties, product specifications and final heat treatment are summarized in [11]. Dimensions of these specimens are not the same: the unirradiated and irradiated specimens of JRQ (Japan Reference Quality) type were in the form of square plates of 10x10x1 mm, otherwise annealed specimens were in the form of rectangle plates of 5x10x0.8 mm. Almost all of JPA specimens were in the shape of square slides with dimensions of 10x10x1 mm except specimens marked as I-2 and I-3, which were in the form of radial discs with diameter of Ø6x1 mm. The effective size of a used source of positrons is about 4 mm and the size and type of the specimens should not influence results and prevent their comparison. A preparation of the all specimens was done in the same process. Specimens were cleaned but they could not be polished due to unavailability of a dedicated preparation chamber. From the surface point of view, some of the specimens were slightly corroded but it should not affect the measurement.

The irradiation of studied Japan model steels was performed in a prototype reactor VVER-210 in Rheinsberg (Germany) at a temperature of 255 ± 5 °C [10] up to three different neutron fluencies for both materials. After the irradiation, the JRQ irradiated specimen I-3 was annealed in six steps with a step value of 25 °C from 350 °C to 475°C. The irradiation and annealed conditions are summarized in Tab. 4.4 and Tab. 4.5.

Tab. 4.4 – Irradiation conditions

Material code	Neutron fluence / 10^{18} cm^{-2} (E > 0.5 MeV)	Flux density / 10^{12} cm^{-2} s^{-1} (E > 0.5 MeV)
JRQ I-1	10	0.15
JRQ I-2	77	3.0
JRQ I-3	139	5.4
JPA I-1	10	0.15
JPA I-2 a-e	80	3.1
JPA I-3	143	5.5

Tab. 4.5 – Annealing conditions of JRQ steel

Specimen	JRQ-I3-A1	JRQ-I3-A2	JRQ-I3-A3	JRQ-I3-A4	JRQ-I3-A5	JRQ-I3-A6
Annealing Temperature [°C]	350	375	400	425	450	475

4.3 Parameters of ion irradiation

The energy of hydrogen ions implantation into P370WM steel was considered at 100 keV and the irradiation was carried out at Linear Accelerator at INPE in Bratislava. The H^+ irradiation was performed in three levels, where the third level is equal to the neutron irradiation in terms of fluence (Tab. 4.6). It is necessary to note that a dose calculated in our experiment is just local value in the layout of the implantation range.

Tab. 4.6 – Overview of implanted parameters of P370W steel

Hydrogen implantation	**Implanted dose [C/cm^2]**	**Fluence [cm^{-2}]**	**Dose in implanted region [dpa]**
1. level	0.10	6.24×10^{17}	1.980
2. level	0.82	5.12×10^{18}	16.235
3. level	3.20	2.00×10^{19}	63.354

Fe^{2+} ion irradiation into as-received JRQ steel was conducted mainly at HZDR at the Institute of Ion Beam Physics and Materials Research. It was part of bigger project focused on the hardening of reactor pressure steels induced by ion irradiation, where six different steels were irradiated by Fe^{2+} ions in Ion Beam Center of HZDR (details of ion irradiation are listed in Tab. 4.7). One of them, JRQ type as specified before, was afterwards studied by means of nanoindentation and Doppler broadening positron spectroscopy with different energies of positrons in order to obtain the depth profile of defects.

Samples of unirradiated material were polished, with diamond paste down to 1 μm particle size before the ion irradiation.

Tab. 4.7 – Fe^{2+} ion irradiation conditions

Specimen	**JRQ 1**	**JRQ 2**	**JRQ 3**	**JRQ 4**	**JRQ 5**
Fluence [cm^{-2}]	2.66×10^{13}	7.98×10^{13}	2.66×10^{14}	7.98×10^{14}	2.66×10^{15}
Exposure [dpa]	0.01	0.03	0.1	0.3	1

5 EXPERIMENTAL TECHNIQUES

5.1 Positron annihilation lifetime spectroscopy

Positron annihilation lifetime spectroscopy is a well-established non-destructive spectroscopic method for evaluation of defect-size (size of vacancy clusters) in materials and its density by positron annihilation intensity of the given lifetime component. Sensitivity of PALS is very high with the ability to detect one defect per 10^7 atoms [12, 13]. These defects cannot be seen by an electron microscope, however PALS can, and in this sense, it provides a unique type of information for microstructural studies of selected materials before and after external treatment (irradiation, annealing, etc.) [9].

Measurement of neutron irradiated steels by PALS was performed by the triple-coincidence method due to the influence of the ^{60}Co [14], which was induced in the steels during irradiation. Nucleus of the ^{60}Co emits two γ-photons with energy of 1173 keV and 1332 keV, respectively, and can be detected as a false start signal. Our PALS set-up is built in an air-conditioned casing with stable temperature. FWHM (Full width at half maximum - resolution of the spectrometer, characterized by a Gaussian) value for our set-up is stable about 175 ps.

5.2 Coincidence Doppler broadening spectroscopy

A measurement of Doppler broadening of positron annihilation spectra is one of the momentum-based techniques, where the momentum of the electron-positron pair is transferred to the photon pair during the annihilation process. The motion of the annihilating pair causes a Doppler shift ΔE of the annihilation energy of 511 keV. This causes the broadening of the 511 keV annihilation line and the measuring of the positron annihilation energy with energy deviations 511 keV $\pm$ ΔE_γ makes possible to characterize the material microstructure at atomic scale, because the non-zero momentum of the electron-positron pairs modify the features of the annihilation radiation [16]. Coincidence Doppler broadening spectroscopy (CDBS) is one of the Doppler broadening spectroscopy (DBS) techniques, which is based on the use of two-detector set-up in order to obtain a second annihilation quantum in coincidence of annihilation events with core electrons. This resulted in an improvement of the peak-to-background ratio by 3-4 orders of magnitude.

The motion of positron-electron pairs prior to annihilation causes Doppler broadening of the photopeak in the measured energy spectrum of the annihilation photons characterized by the lineshape parameter S. S is higher for positrons trapped at and annihilated in open-volume defects (corresponds to positron annihilation with valence electrons) and it is sensitive to size and concentration of vacancy-like defects. The W parameter ("wing" or core annihilation parameter) is taken at the high-momentum region away from the center. Since the positron annihilation takes place with core electrons, the W parameter probes the chemical surrounding of the annihilation site. The parameters S and W are calculated as the normalized area of the curve in a fixed energy interval. The correlation between both parameters varies for different defect types [13].

5.3 Slow-positron DBS

Positrons from the conventional positron sources can reach a depth around ~100 μm in the metallic materials and forasmuch as positrons are created in various energies, they annihilate also in various depths, which brings the information about the material properties from the surface up to the depth of ~100 μm. This relatively high depth penetration of positrons cannot provide exact information from a one specified depth. This is why, monoenergetic positrons are needed to make possible near-surface or defects profiling investigations. Monoenergetic positrons are reached by moderation, and then the linear accelerator is used to obtain the specified energies.

Slow-positron beam system "SPONSOR" (The Slow-Positron System of Rossendorf) at Helmholtz-Zentrum Dresden-Rossendorf (HZDR) was used in the experimental investigation of the RPV steels in this thesis. Positrons from the source (^{22}Na) are moderated using a tungsten foil and pre-accelerated to 30 eV in the beginning of the SPONSOR. Since the moderation efficiency of tungsten is in order of 10^{-4}, most of the positrons are still fast positrons. Due to this, a bent tube is used to separate fast and slow positrons. The bent tube is magnetically adjusted in that way, that only slow positrons with defined kinetic energy can pass through. After the bent tube, the slow positrons are usually accelerated to energies up to 36 keV. Then the positrons are magnetically still guided to the sample, which has a distance from the source of 3 m. Helmholtz coils and solenoids create an axial magnetic field of 10 mT. The annihilation events are recorded with two Germanium detectors facing each other with an energy resolution of 1.09 ± 0.01 keV [14].

5.4 Nanoindentation

Nanoindentation is used for measurement of the hardness in very thin specimens or in shallow depths under the surface. This technique is a very precise device operating in sub-nanoscale based on pressing an intender tip into the sample surface. The tip is made of a very hard material (usually diamond) whose mechanical properties are known. An increasing load (up to desired value) within a related displacement is recorded, which results to a production of a load-displacement curve. A loading

part of curve describes elastic-plastic properties of material and an unloading curve describes only elastic properties of the measured material. The layer of the measured material should be at least ten times larger than the indent depth. Afterwards the load is removed an indent is leaved in the sample surface

The nanoindentation testing was performed using the Universal Nanomechanical Tester (UNAT, Advanced Surface Mechanics GmbH, now part of the Zwick-Roell Group) equipped with a Berkovich indenter. The calibration of the indenter area function and the instrument stiffness was done based on measurements on two reference materials (fused silica, sapphire) with known elastic modulus [15]. Although the ion irradiation is a very advantageous method for the study of radiation damage, the damage itself from ions is localized only in a surface layer in depth up to several micrometers. When we want to measure the hardening (or other problems related to steels such as creep, elasticity, stiffness etc.) of materials due to the ion irradiation, only the irradiated layer must be investigated to obtain relevant results. This is the reason why the nanoindentation must be used for this kind of investigation and it is the lead powerful tool for qualitative analysis of the impact of ion implantation.

6 RESULTS

6.1 PALS results of neutron irradiated German RPV steels

All three specimens of P370WM steel (two irradiated D77 and D161, as well as one non-irradiated CD159) are from the same bulk but were cut at different positions. The same is valid also for both P16WM specimens (S103 and GS67). Unfortunately, there was no unirradiated specimen from P16WM material.

Average positron lifetime (τ_{avg}) is calculated from measured data and includes only annihilations in material, components τ_1 and τ_2 with their intensities I_1 and I_2 ($\tau_{avg}= \tau_1.I_1+\tau_2.I_2$). This parameter provides complex information about defect size. Average positron lifetime was chosen to interpret the qualitative characterization of steels prior to using of Mean Life Time ($MLT= \tau_1.I_1+\tau_2.I_2+\tau_3.I_3$) due to large difference of parameters τ_3 and I_3 in our specimens because of various shapes of them (I_3 ~ 0.4-7%, τ_3 ~ 680-2300 ps). It was proven that the performed irradiation caused an increase of the positron lifetime in studied specimens. In the case of both specimens of P370WM steel, the increase of τ_{avg} parameter was from 143±0.7 ps to 157±0.7 ps and 147±0.2 ps, respectively (Fig. 6.1). Results obtained for τ_{avg} parameter were at a level around 172±1 ps for both P16WM specimens.

The positron lifetimes in defects, characterized via parameters τ_2 and I_2, are given in Fig. 6.1 and Fig. 6.2. In the case of P16 WM steels, τ_2 is at levels of 196±4 ps (GS67) and 197±1 ps (S103), respectively. This indicates a presence of small vacancy clusters with the size of 1-2 vacancies. In the case of the P370 WM steel, the lifetimes in defects are higher with values of 203±8 ps (D77) and 213±3 ps (D161), respectively. It can indicate the size of vacancy clusters around 2-3 vacancies [16-19].

A look to data of intensities (Fig. 6.2) shows that intensities of second component assigned to defect component (I_2) of P16 WM steel of high Ni (1,69 wt%), low Cr (0,07 wt%) and low Cu (0.08 wt%), are at a level around 77%. In the case of P370 WM steel with relatively low Ni (1.11 wt%) but high Cr (0.74 wt%) and Cu (0.22 wt%), intensities of defects are much lower (50-51%) but the lifetimes in defects are higher. Thus, it can be assumed here that smaller defects (dislocation lines, mono- and mostly of divacancies) in a relatively high amount are more homogeneously distributed in the microstructure of P16WM steel than in P370WM. Bigger defects (mostly 2-3 vacancies) in P370WM are not so homogeneously distributed if it is approached that they are approximately evenly distributed in the whole volume of the material. This can be due to Cu precipitation after the irradiation, where defects are associated with Cu-rich precipitates. A larger difference of I_2 between D77 and D161 of P370WM could be caused due to a significant difference of the activity of both of samples (although that fluence is almost the same (Tab. 4.2). Unfortunately, the exact conditions of the irradiation are not

known and it is hard to say why it is. Here should be also mentioned that P370WM steel belongs to the 1st generation of German PWRs and P16WM steel belongs to 3th generation.

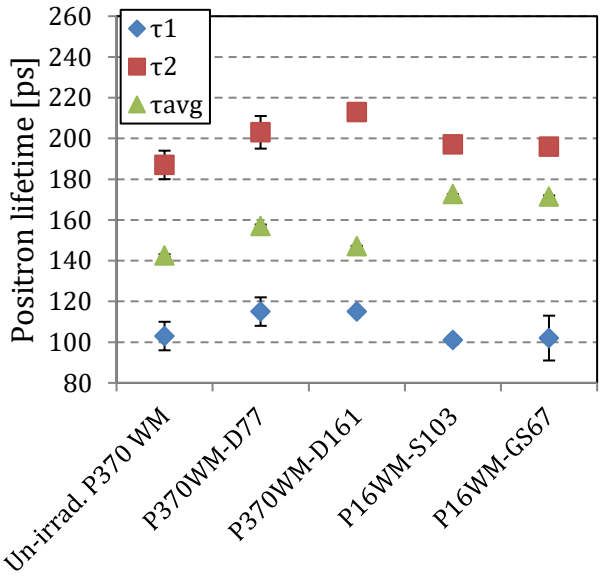

Fig. 6.1 - Positron lifetimes of neutron irradiated German RPV steels

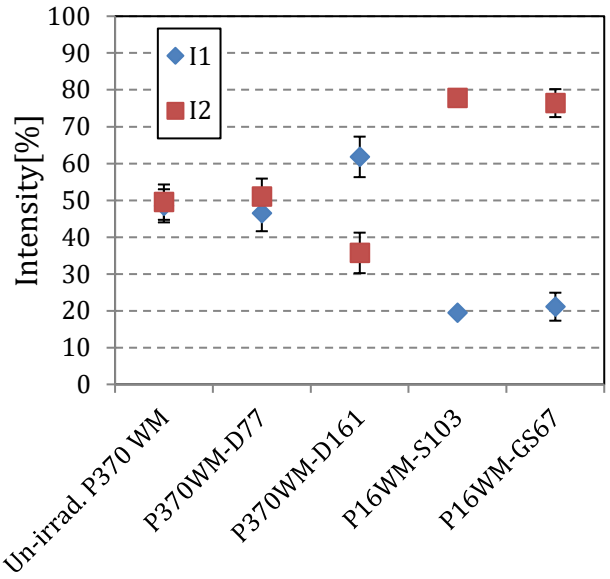

Fig. 6.2 - Intensity of positron lifetimes of neutron irradiated German RPV steels

6.2 PALS results of H^+ ion irradiated P370WM steel

After H^+ irradiation of the P370WM virgin sample, it was measured, and results were obtained that the positron lifetime in defects (τ_2) increased predictably (Fig. 6.3). In the case of the first level of implantation the defect component increased from 187±7 ps to a value of 214±12 ps. At the second level of implanted dose τ_2 is about 215±7 ps. According to the theoretically calculated values [20], this lifetimes in defects indicate the presence of defects with the size of about 2-3 vacancies. The third level of implantation significantly shows a growth of the vacancy size up to a value of 238±10 ps, which shows that larger vacancy clusters are present in the H^+ irradiated material with the size of 3-vacancies.

Results of average positron lifetime show an increase with all increasing accumulated doses due to the H^+ irradiation. From as-received 143±0.7 ps to 147±0.5 ps of the first level, 148±0.3 ps of the second level and finally to 151±0.4 ps of the third level of implanted doses, respectively. Based on an analysis of the measured intensities of annihilation components (Fig. 6.4), there can be seen a decrease of the intensities of the defect component (I_2) by more than 10-20% in the implanted samples. With knowledge of the defect size behaviour after the H^+ ion irradiation (Fig. 6.3), it can be concluded that defects on open-volume (vacancy) levels began to accumulate into larger clusters, through a reduction of the intensities of annihilations in defects and an increasing of the intensities of annihilations in bulk.

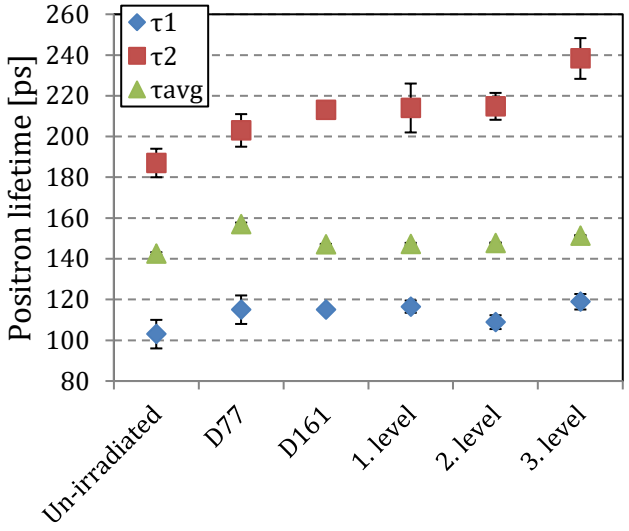

Fig. 6.3 - Positron lifetimes of all measured P370 WM specimens – unirradiated, neutron irradiated (D77 and D161) and 3 levels of H+ ion irradiated

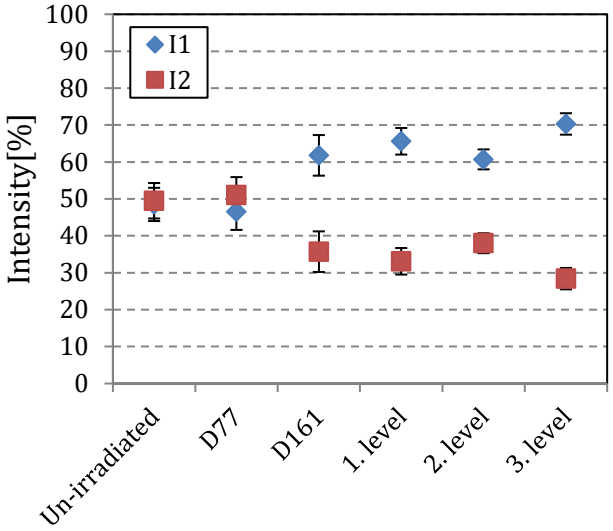

Fig. 6.4 - Intensity of positron lifetimes of all measured P370 WM specimens – unirradiated, neutron irradiated (D77 and D161) and 3 levels of H+ ion irradiated

Average positron lifetime of the neutron and H^+ ion irradiated specimens, compared to the unirradiated state, increased slightly or stayed at the similar level. This fact can be interpreted as the damage caused by irradiations did not induce a significant increase in the defect size and a change of physical and mechanical properties of the material.

6.3 PALS results of Japan JRQ steel

In unirradiated state of both steels the main defect type corresponds mainly to divacancies (205±13 ps for JRQ and 201±8 ps for JPA, respectively), which were formed during the manufacturing. JRQ steel is a low-copper alloy in our case. There is a prediction that low-Cu steels should have been less sensitive to the creation of induced-defects caused by neutron irradiation [21]. The well-known hardening effect is more pronounced for the specimen materials with higher Cu [10].

The positron lifetimes in the defect component increased significantly by the influence of neutron irradiation just in the first irradiated specimen I-1 (Fig.) to level of 3-4 vacancy clusters (248±25 ps). The defect component of other two irradiated specimens (I-2 and I-3) stayed at the similar value of divacancies (209±11 ps for I-2 sample and 218±19 ps for I-3 sample). However, if the implications of positron lifetimes intensities, which correspond to the amount of defects in the crystal lattice, are considered (Fig.), there will be able to see that the specimen I-1 has a smaller amount of larger defects (~23%) as other irradiated JRQ specimens (~42-45%).

The general behaviour of defects accumulation in materials is described by average positron lifetime. It was proven that the performed irradiation treatment caused the increase of average positron lifetimes in studied specimens. In the case of the JRQ specimens, the τ_{avg} parameter increased slightly from unirradiated 163±1.5 ps to 165.5±2 ps, 168±1.5 and 168.5±2.5 ps, respectively (Fig. 6.5), but it is just an indication of the increase because the variations are within the error bars.

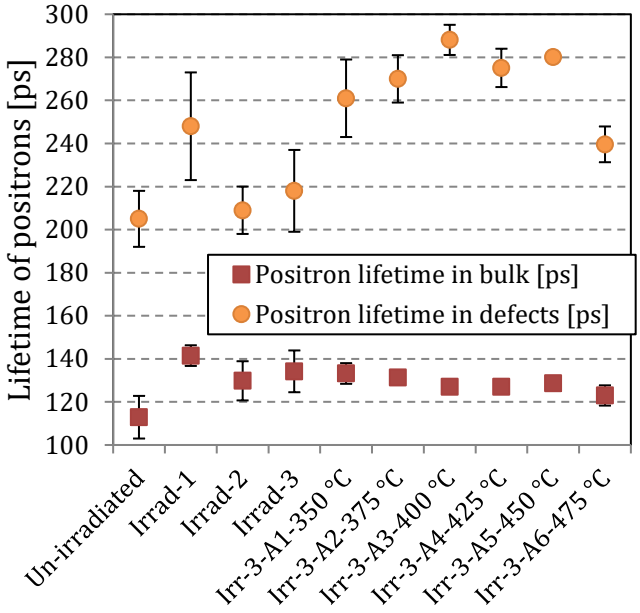

Fig. 6.5 - Positron lifetimes of the JRQ specimens

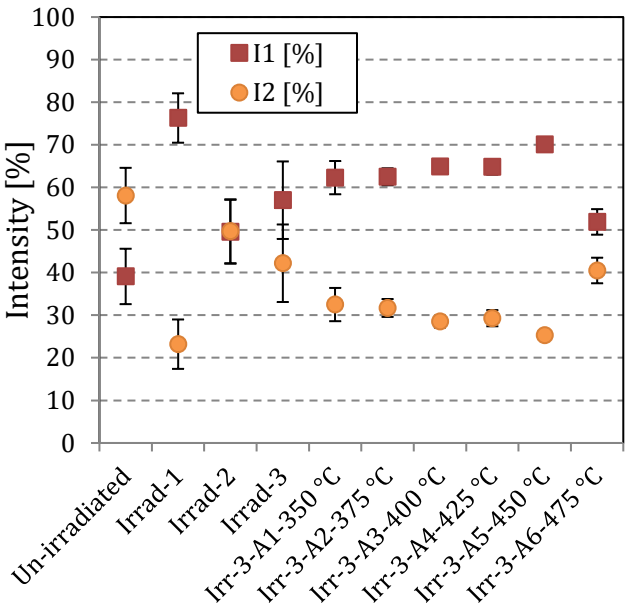

Fig. 6.6 - Intensity of positron lifetimes of the JRQ specimens

The JRQ specimens were also annealed in six steps from 350 °C to 475 °C. From the defect size point of view, it was observed the increase in lifetime of defects up to 288 ps in Irr-3-A3 specimen. This value could indicate the presence of mostly 5-6 vacancy clusters. Lifetimes of positrons in defects in other annealed specimens are approximately 260-280 ps, which correspond to 4-5 vacancy clusters. The lifetime in defects of the last annealed specimen Irr-3-A6 dropped to 240±8 ps, which indicate the presence of mainly 3-4 vacancy clusters. Intensities of defect annihilations after the annealing (Fig. 6.6) decreased from 33% to 25% except for the last annealed specimen Irr-3-A6, where intensity in defects (I_2) reached again 40%. The last annealed specimen showed a different behaviour during the annealing than other annealed specimens. Defects began to create smaller vacancy clusters within the increase of intensity of the defect component. An explanation can be in a dispersion of larger defects into the volume of the steel due to higher annealing temperature (475 °C is close to the ideal temperature of a commercial annealing of PWR reactors – mostly VVER types).

If average lifetime of positrons is examined, a significant decreasing trend during the annealing after the irradiation will occur in all annealed specimens. Slugeň et al. summarizes in [22] the comprehensive PALS study involving an annealing of non-irradiated RPV including JRQ up to 800 °C and from MLT point of view the trend was quite comparable with our τ_{avg} parameter because both of them have a decreasing trend within temperature. The size of the defects and their intensities are shown that after the annealing, small defects were coalesced into bigger defect clusters except in the case of the last annealed specimen.

6.4 PALS results of Japan JPA steel

JPA steel is considered to be a high-copper alloy with the prediction that higher Cu content should have been responsible for the stronger neutron-induced embrittlement. Positron lifetime in defects (Fig. 6.7) increased from unirradiated value of 201±8 ps, which corresponds to divacancies, to values of around 251-270 ± 10 ps (mostly 3-4 vacancy clusters) in specimens I-2a – I-2e (five different cuts of the same irradiated material) irradiated with fluence of 8.0 x 10^{19} cm^{-2}. The same component τ_2 increased in I-1 and I-3 specimen to values of 299±12 ps and 283±6 ps, respectively (mostly 5-6 vacancy clusters).

Intensities of defect components (Fig. 6.8) decreased from unirradiated state from 49% to 24% in the I-1 specimen and to 36% in the I-3 specimen. The set of five comparable specimens I2-a till I2-e have decreased to values about 38%. It should be mentioned that I-1 and I-2 were in the form of radial discs with the high corroded surface layer, which could be responsible for the higher defect sizes. Also, in JPA steel the agglomeration of smaller defects to bigger clusters occurs.

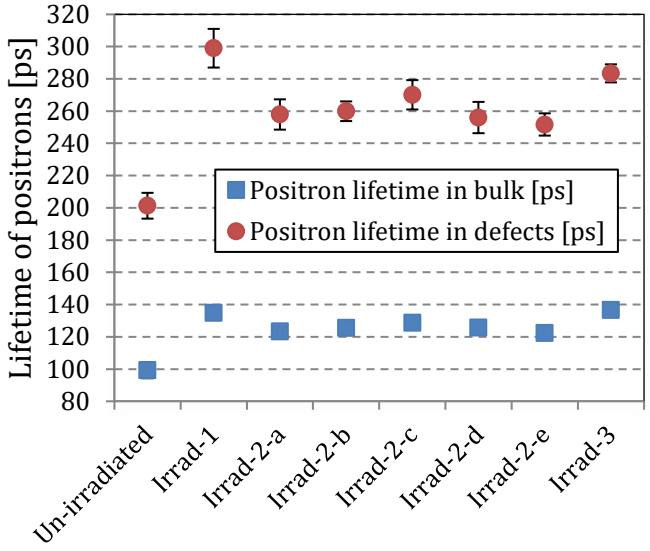

Fig. 6.7 - Positron lifetimes of the JPA specimens

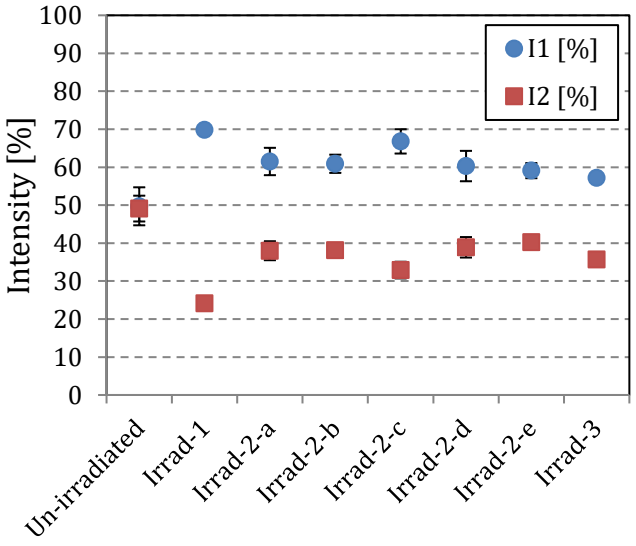

Fig. 6.8 - Intensity of positron lifetimes of the JPA specimens

6.5 Comparison of JRQ and JPA steels from PALS point of view

Positron measurements show that di-vacancies are the most effective positron traps in the as-received specimens. After applying three different irradiation fluences to JRQ steel the lifetime of positrons increased creating clusters of 3-4 vacancies or did not increase in size, rather in intensity. After the annealing the defect size increased to clusters of 5-6 vacancies, however the intensity of positrons annihilating in these defects is relatively low (25-30%). This could indicate the presence of agglomerations of bigger clusters, which emerged during the annealing. In the case of JPA steel the defect size increased from di-vacancies to clusters of 3-4 vacancies. Measurements indicate that the radial specimens of JPA steel might include also larger defects of 5-6 vacancies.

The best way to compare the investigated steels is use average positron lifetime (Fig. 6.9), which can be interpreted as a qualitative PALS parameter. As-received specimens of our steels show that the JPA specimen has a lower value of τ_{avg} parameter than JRQ. A steel quality before the irradiation depends mainly on a manufacturing process like rolling, heat treatment, quenching and tempering, etc. Whereas, an exact manufacturing process of the studied specimens are not known, the lower τ_{avg} value of JPA steel does not define any difference of a quality of the steels in the as-received state.

After the irradiation, the τ_{avg} increased in both steels but the increase is much more significant in JPA steel. Relatively small fluence (1.0×10^{19} cm^{-2}) caused rapid increase of τ_{avg} in the JPA specimen. In both steels of the irradiated specimens I-1 the values of τ_{avg} are almost the same. Continued irradiation of JPA steel shows higher values of τ_{avg} than in JRQ steel but the increasing trend of τ_{avg} is smaller with higher fluences (up to 7.7 and 13.9 $\times 10^{19}$ cm^{-2}). The deviation in τ_{avg} of JRQ and JPA steels after third level of irradiation (I-3 specimen, fluence ~14.0×10^{19} cm^{-2}) is almost 10ps with less than 2ps error. It can be stated that JPA steel is more sensitive to neutron irradiation-induced creation

of defects than JRQ steel. This behaviour what was expected due to higher copper Cu content of JPA steel, where the high copper and high temperature condition is dominated by Cu precipitation, which was confirmed for JPA steel by Boydon et al. [23]. Debarberis shows in [2] that an essential part of neutron damage in steels, from a DBTT point of view, is caused in the beginning of the irradiation - mostly due to precipitation of Cu in the crystal lattice. Copper atoms precipitate to the grain boundaries due to the irradiation, where the movement of dislocations is hindered by solute obstacles, which are responsible for the embrittlement of the material. A created stress around grain boundaries is increasing hardness and also supporting the creation of bigger vacancy clusters during the irradiation [23]. This approach is in the coincidence with our results of the measured specimens with higher Cu content.

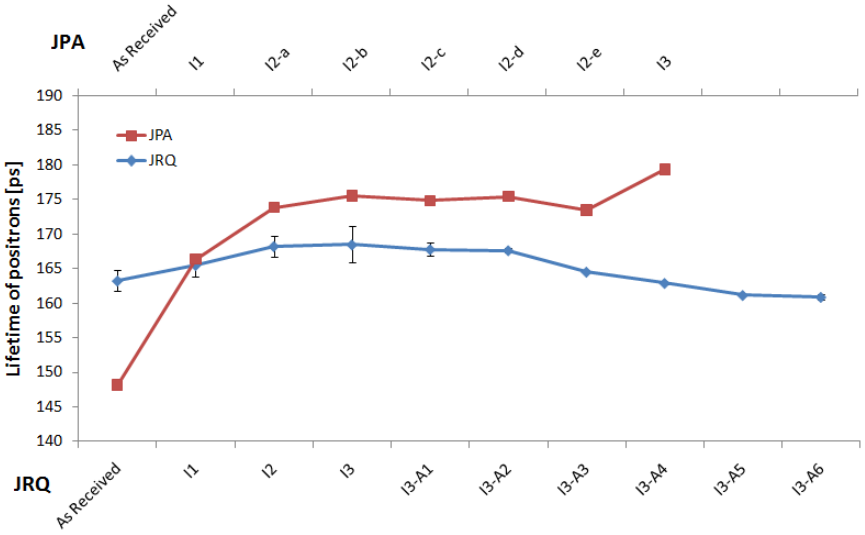

Fig. 6.9 - Average positron lifetimes of the JRQ and JPA specimens

6.6 CDBS results of JRQ steel

CDBS measurement was done just for JRQ steel because there was a strong interest in this steel in order to obtain a huge comprehensive database of experimental data for this kind of steel. Results are shown in Tab. 6.1.

Tab. 6.1 – CDBS results - S and W parameters and values normalized to the unirradiated value

Specimen	Unirrad.	I-1	I-2	I-3	I3-350°C	I3-375°C	I3-400°C	I3-425°C	I3-450°C	I3-475°C
S parameter	0,3518	0,362	0,365	0,364	0,366	0,363	0,362	0,358	0,361	0,362
W parameter	0,0314	0,030	0,029	0,029	0,029	0,030	0,032	0,033	0,032	0,030
S/S_{ref}	1	1,030	1,038	1,035	1,041	1,032	1,028	1,018	1,027	1,029
W/W_{ref}	1	0,949	0,917	0,930	0,913	0,969	1,020	1,048	1,015	0,963

In Fig. 6.10, there are shown parameters S/S_{ref} and W/W_{ref} in order to see better a difference between them. The S/S_{ref} parameter (qualitative parameter sensitive to open volume defects) increases rapidly after the first level of irradiation and then the slope becomes less rapid and even decreases slightly in the third irradiated specimen. The annealing provides an observable decrease after the first annealing level of 350 °C during the whole procedure, even if it seems that the first level of annealing caused a small increase of S parameter compared to the third level of irradiation – defects could arise slightly. The lowest value of S/S_{ref} occurs at the temperature of 425 °C what is followed by slight increase of the parameter. The S/S_{ref} parameter behaviour showed here can be interpreted as in accordance with our PALS results and can be compared to each other.

The W/W_{ref} parameter (sensitive to the chemical surrounding at the annihilation site) behaviour is exactly the same as in the S/S_{ref} but in opposite direction. Information about chemical surrounding is obtained from core electrons annihilations, which are reciprocally sensitive with higher annihilations with valence electrons. However, a total difference from 1 is two times larger in the W/W_{ref} parameter

($\Delta \approx 0.083$) as in the S/S_{ref} parameter ($\Delta \approx 0.038$) if look at the second level of irradiation. This can be interpreted as the irradiation had a stronger influence (damage) to induced changes in chemical aspect of the steel (e.g. precipitations, segregations of particles, transmutation...) than to creation of open-volume defects. Similarly, the annealing effect was observed stronger by W/W_{ref} parameter than S/S_{ref}.

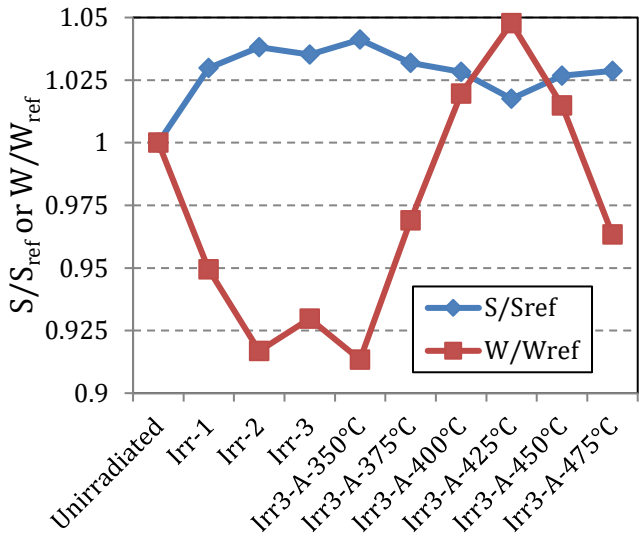

Fig. 6.10 – S/S_{ref} and W/W_{ref} parameters of CDBS

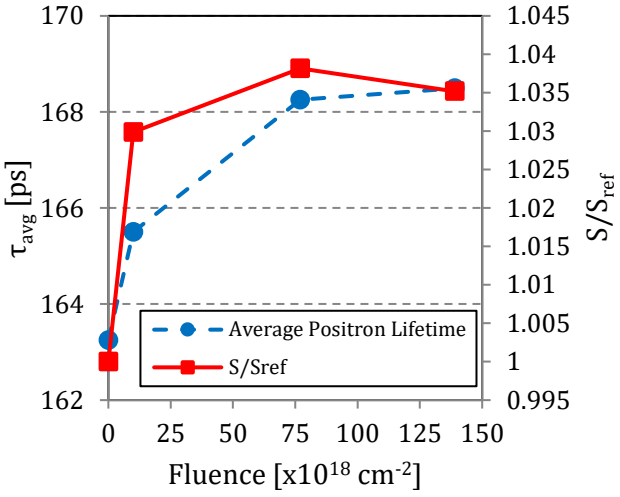

Fig. 6.11 - Irradiation dependence of average positron lifetime and S/S_{ref} parameter of PAS techniques

Fig. 6.11 shows the irradiation dependence of τ_{avg} and S/S_{ref} parameters. As can be seen, the behaviour of both, the τ_{avg} and S/S_{ref}, as a function of the fluence is very similar. There is an observable increase in the both of defect dependent parameters. Slight difference can be noticed after the second level of irradiation, where τ_{avg} is lightly still increasing and vice versa S/S_{ref} parameter is lightly decreasing. Both techniques are suitable non-destructive complementary methods, but they are not usually used at once and compared to each other. During the neutron irradiation the agreement of both PAS techniques have been very good and convincing.

6.7 Effectiveness of annealing by PALS and CDBS

JRQ steel after the irradiation with fluence of 139×10^{18} cm^{-2} was annealed in six levels as specified before – Tab. 4.5. PALS measurement was done at the annealed samples and an effectiveness of annealing was investigated. It is quite hard to interpret data incorporating the size of defects or intensities in order to see some kind of trend of these parameters as a function of annealing temperature. For this reason, an interpretation of results is based on average positron lifetime τ_{avg}, which provides qualitative view on the investigated specimens from PALS point of view. In Fig. 6.12 is shown temperature dependence of the τ_{avg}. It is clearly seen that τ_{avg} decreases with increasing annealing temperature up to final temperature of 475 °C. In this range, the annealing provides a noticeable improving of the material from PALS point of view. From literature [25-29], this range of temperatures and especially temperature of 475 °C is recommended for dry thermal annealing of RPVs. After this temperature, benefits of annealing lose their significance on RPVs. Also Slugeň found out in [30] that ideal annealing temperatures are between temperatures of 450-475 °C and annealing after about 500 °C brings a rapid increase of small defects in Russian type of RPV steels (Sv-10KhMFT – Russian weld steel of VVER-1000). Unfortunately, it is not evident from our results if such behaviour could occur in JRQ steel after annealing temperature of 475 °C, but most likely it should.

During the third level of neutron irradiation the τ_{avg} parameter increased from unirradiated level of 163±1.5 ps to 168.5±2.5 ps. Annealing provides decrease of the τ_{avg} up to 161±0.5 ps. Already at temperature of 425 °C the τ_{avg} reached (163±0.5 ps) the value of unirradiated specimen. It seems, from

PALS point of view, that the annealed JRQ steel from 450 to 475 °C has a smaller number of defects (to be more specific: a bit bigger defects but with smaller intensity – from Fig. 6.5 and Fig. 6.6).

In Fig. 6.13 can be seen the behaviour of τ_{avg} and S/S_{ref} as a function of the annealing temperature of irradiated JRQ steel after third level of the irradiation ($139x10^{18}$ cm^{-2}). τ_{avg} parameter has the decreasing tendency with all the annealing temperature range. Otherwise, S/S_{ref} parameter decreases just up to 425 °C, after that increases over again with very similar rate as in the decrease. Although during the first four annealing steps is observable a similar behaviour, the last two steps shows an anticoincidence. From this point of view of PAS techniques, an ideal temperature of annealing seems to be 425 °C by CDBS and 475°C by PALS results (for annealing of RPV steels is currently recommended temperature around 475°C [25, 26]). The process of embrittlement of the RPV steels is not just caused due to evolution of vacancy type defects. This process is much more complicated and broader. In JRQ steel with not insignificant amount of Cu in the chemical composition, other effects influence embrittlement – mostly Cu segregation and clustering [25].

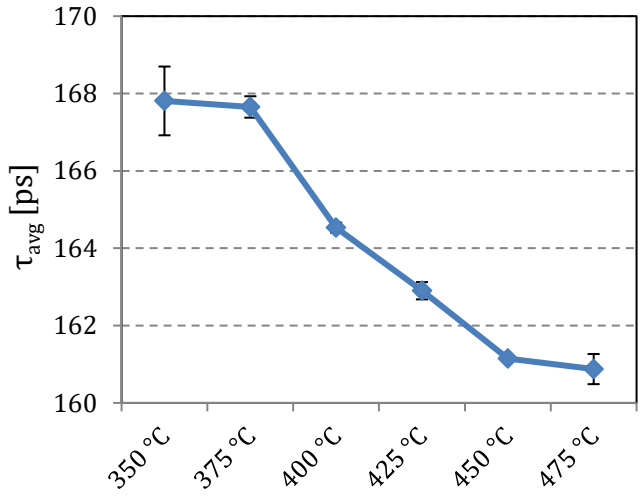

Fig. 6.12 – Temperature dependence of the average positron lifetime in the annealed JRQ samples

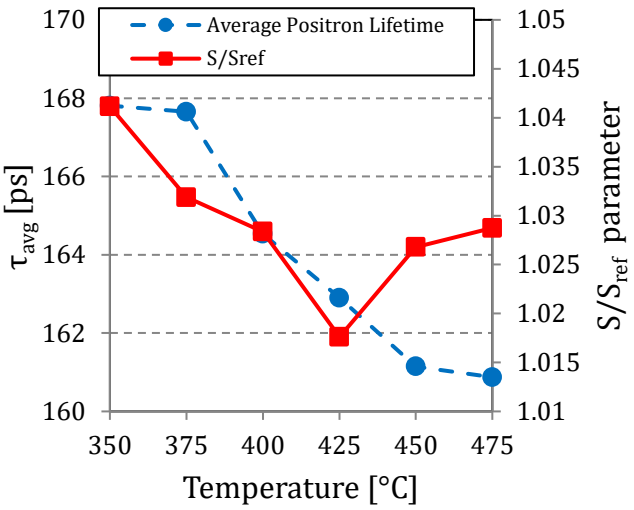

Fig. 6.13 - Annealing temperature dependence of average positron lifetime and S/S_{ref} parameter of PAS techniques

This difference can be caused by various reasons. Both PAS techniques are sensitive to vacancy type defects, but in the case of the annealing, second part of the plot shows a clear discrepancy.

6.8 Slow-positron DBS results

Slow-positron DBS measurement was done on the SPONSOR facility at Institute of Radiation Physics of HZDR. The SPONSOR with an energy resolution of the two Germanium detectors of 1.09 ± 0.01 keV at 511 keV can modulate the energy of positrons, which leads to a depth profile of Doppler broadening of the positron annihilation spectrum [13]. Magnetically guided positrons from a ^{22}Na source of predetermined energies E (30 eV – 36 keV) were implanted at depths of up to a few micrometer in the sample. The parameters S and W are calculated as the normalized area of the curve in a fixed energy interval. The correlation between both parameters varies for different defect types [13].

Results obtained by slow-positron DBS are shown in Fig. 6.14. About $6x10^5$ measured counts belong to each measured energy of DBS. Errors of slow-positron DBS measurement of S and W parameters was less than 1%. There is a significant increase of S parameter (Fig. 6.14a) after each step of the Fe^{2+} ion irradiation, when comparing the experimental data with those obtained for the

unirradiated material. S parameter, representing open volume defects as a qualitative parameter, increased as a function of incident positron energy and made a slight indication of a peak around energy of 20 keV, which should occur on area of the maximal damage in depth around 1.3 μm. This peak can be seen much better in plot of S/S_{ref} (Fig. 6.15), where S_{ref} is the S-parameter obtained for the unirradiated material as a function of energy. Differences in the irradiated specimens are very small and whereas the first fluence (0.01 dpa) is the smallest one, other S parameters of irradiated specimens are almost the same.

But If one looks more precisely to the S(E) plots it is seen that the S parameter is increasing with increasing fluence till a damage of 0.1 dpa. With 0.3 dpa the same damage level as in case of 0.1 dpa is reached. However, with a damage of 1.0 dpa a certain "self-annealing" is reached which is reflected - in a decreasing S parameter to the same level of S as in case of a damage of 0.03 dpa and in a longer positron diffusion length than for 0.1 and 0.3 dpa. The positron diffusion lengths in the 0.03 dpa and 1.0 dpa damaged samples are nearly the same, which is a further hint that the damage in both samples is from the same level. On the other hand, increasing of S parameter in unirradiated-reference specimen as the positron energy decreases is due to a shallow surface depth, where a greater amount of open volume defects is presented (higher S parameter). Over the positron energy of 20 keV, S parameter of reference material became saturated. For irradiated specimens there is also an obvious bigger formation of vacancy-type defects close to the sample surface (~ below energy of 10 keV). Furthermore, the damaged range becomes broader and moves to the surface with increasing damage, especially seen in the difference of S between 8 and 14 keV. The smallest damage range is measured for the low fluence sample 0.01 dpa.

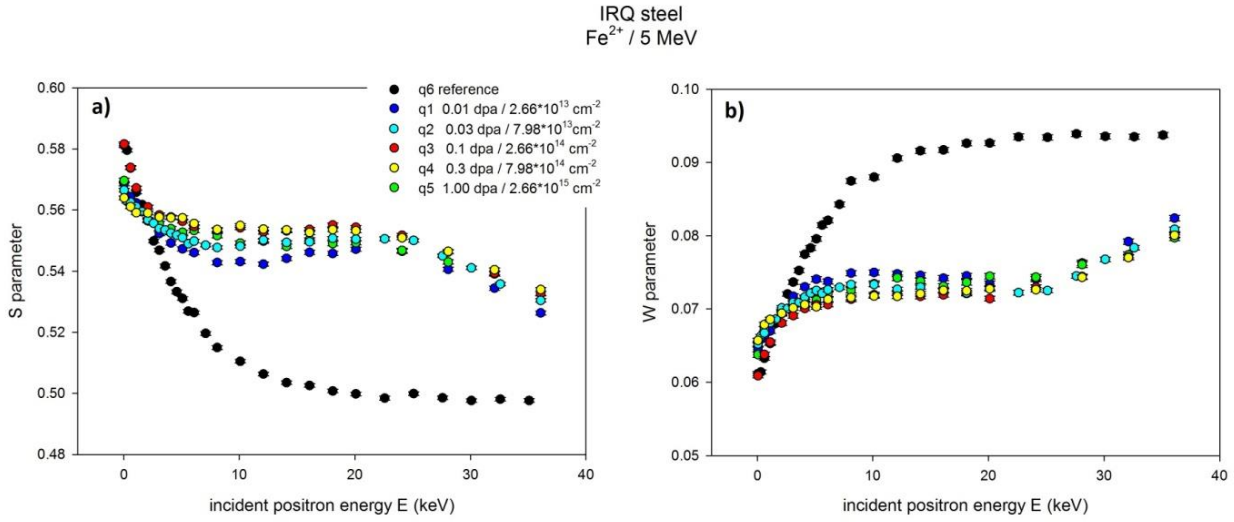

Fig. 6.14 - S (a) and W (b) parameter of slow-positron DBS as a function of positron energy

From slow-positron DBS results can be stated that here is no significant change of open volume defects with higher doses of Fe^{2+} ion irradiation. Vacancy concentration reaches a saturation level already at 0.01 dpa and then remains approximately the same, which means that defect concentration is independent of the dpa levels. Nevertheless, this saturated vacancy concentration is enough for Cu atoms to diffuse. Unfortunately, the specific size or amount of these defects from DBS technique cannot be derived.

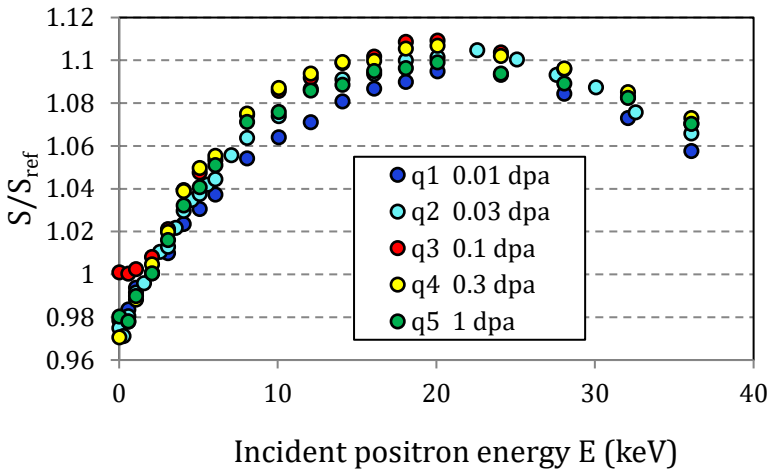

Fig. 6.15 - S/S_{ref} as a function of incident positron energy

6.9 Nanohardness testing

Each of single measurement of nanoindentation hardness was done in square array of 6x6 indents, where has been obtained 35 usable indents (the first one is for the calibration of measurement). A sharp Berkovich indenter tip was used. Indents were made close to the edge of the irradiated circle area, due to further DBS measurements. All the measurements were done as Quasi-Continuous Stiffness Measurement (QCSM), where maximum force of indents was set-up to 50 mN, which corresponds to the indentation depth up to 900 nm (in the unirradiated sample). An average load displacement curve is calculated from the single corrected curves of more than 10 indents which were placed in a regular array with a spacing of 50 μm to avoid interference by neighbouring indents. To calculate the average curve, the load or holding time in case of the holding segment, is divided into intervals. The data points of all curves within this interval are averaged. Data analysis is done by means of a method developed by Doerner and Nix [31] and improved and adapted to pyramidal indenters by Oliver and Pharr [32, 33].

In order to compare the irradiation-induced hardening for different irradiation conditions, the hardness values at a reference indentation depth of 200 nm were selected from previous measurements and experiences, because there is not yet significant influence from the softer substrate of material. As Oliver and Pharr showed [32], the extent of the plastic zone beneath an indenter tip is dependent on several material parameters; typical values of plastic zone radius are reported to be in the range of 4–10 times the indentation depth. It is important to note that, for this reference depth, the whole indented volume is unaffected by injected self-interstitial atoms. Moreover, 50% of the volume of the plastic zone (assumed to extend 7 times deeper than the indentation itself as suggested by Heintze [34]) are also unaffected by injected self-interstitial atoms. The factor of 4-10 by Oliver and Pharr is consistent with the factor 7 used by Heintze.

The measured results of nanoindentation for JRQ steel are shown in Fig. 6.16. There is a clear increase of indentation hardness with an increase of fluence. While the hardness of unirradiated JRQ sample decreases slightly beyond an indentation depth of 200 nm due to the well-known “indentation size effect” [35] as specified below, hardness of all irradiated samples increased above unirradiated material at lower indentation depths mostly. An increase in hardness tends towards the unirradiated bulk value at higher indentation depths, when a plastic zone of the indent extends beyond the damage layer into the softer unirradiated bulk [36]. The well-established indentation size effect (ISE) [35] is observed and presented in all measured fluencies (ISE is mixed with the irradiation effect except for the unirradiated sample), which can be seen as slight hardness values increase as the indentation depth decreases [36]. This is likely to be caused by an increase in stress required for plastic deformation in small volumes (large strain gradient in small indentations), which is seen as the slight increase of

hardness values as the indentation depth decreases. The maximum load of 50 mN corresponds to indentation depths of about 0.89 μm and 0.79 μm for the unirradiated and ion irradiated conditions of the highest exposure (1 dpa), respectively.

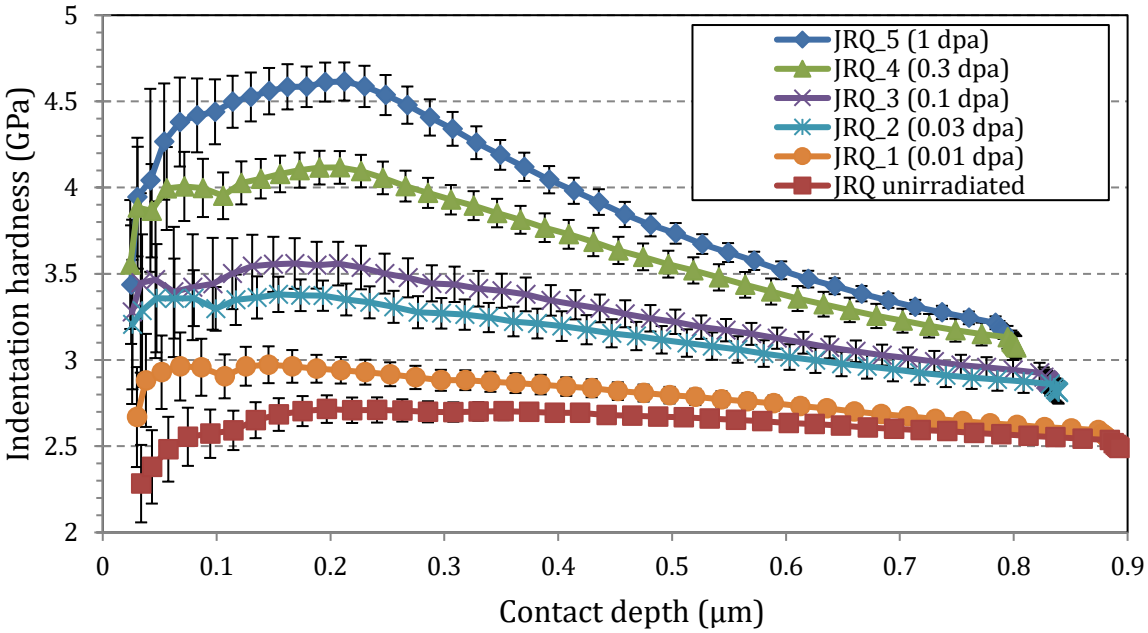

Fig. 6.16 - Indentation hardness as a function of depth

The hardness values at a reference indentation depth of 200 nm were selected in order to compare the irradiation-induced hardening for different irradiation conditions. The reference depth was selected as a compromise between increasing errors at smaller depths and increasing substrate effect at larger depths. The hardness in some cases decreased below 200 nm (Fig. 6.16) and the errors increase considerably. The indentation hardness H_{IN} values taken at the reference depth of 200 nm are 2.71 GPa, 2.95 GPa, 3.35 GPa, 3.53 GPa, 4.09 GPa and 4.62 GPa, for the unirradiated sample and all irradiated samples with increasing fluence, respectively. These hardness values are presented in Fig. 6.17 as a function of fluence, where can be seen that the hardness increases rapidly after the first two fluencies. Then it becomes less rapid, but saturation is not yet reached in the covered dpa range.

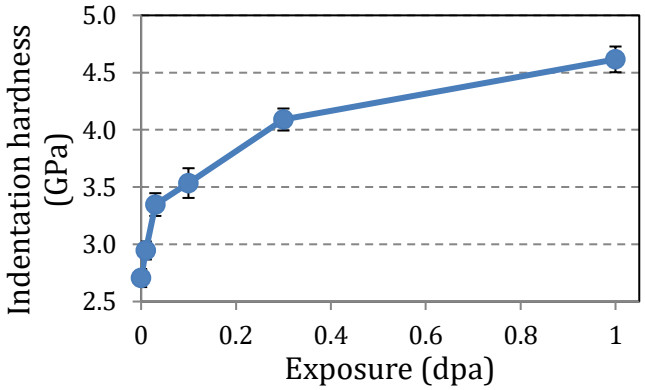

Fig. 6.17 - Hardness in the reference depth of 200 nm as a function of fluence

The decrease of hardness below 200 nm (Fig. 6.16), which has made even an indication of a peak, is most likely explained by Fischer-Cripps [37]. He brings an explanation that the initial rise in hardness, in most cases and especially in very hard materials, is entirely expected on the grounds that the indenter tip, at this scale of testing, is initially round and so the contact is mainly elastic. Further, he says the value of hardness calculated under these conditions, is the mean contact pressure, which, for a given load, will be less than the hardness of the specimen material. Once there is a fully developed plastic zone, the hardness of the film should reach a constant or plateau. At larger loads, or greater

depths, the influence of the substrate will then be felt. Later, the ISE will become much more significant. This is the reason that it is important to use the sharpest possible tip when one desires to measure the hardness of a very thin film.

6.10 Discussion about Fe^{2+} irradiated JRQ steel

There is a rapid nanohardness increase in ion irradiated JRQ up to approximately 0.03 dpa and then a slower increase (Fig. 6.17). After this slower increase, surprisingly, the dependence does not indicate saturation in the range of measurement. On the other side, open volume defects increased after the irradiation but remained at the same level from S parameter point of view (Fig. 6.14). One of the conclusions is that major part of open volume defects (most probably vacancies and small vacancy clusters) were created during the ion irradiation after the first exposure. The concentration of these defects is much higher than the vacancy concentration at thermal equilibrium and seems to be saturated at approximately 0.03 dpa. While these defects are responsible for the irradiation-induced microstructure evolution via irradiation enhanced diffusion, they do not contribute significantly to the irradiation-induced hardening because of the small size of defects.

If there is an assumption that plastic zone is a half sphere with center at the surface and plastic zone radius is seven times indentation depth (200 nm in our case) [34], then the volume of the plastic zone will be 5.75 μm^3. According to our SRIM calculations, which were described in section 2, there are almost no SIAs up to the reference depth of 0.5 μm. The volume of that SIA-affected part of the plastic zone is 2.8 μm^3 and the unaffected part is 5.75-2.8 = 2.95 μm^3. This means that approximately 50% of the plastic zone volume is unaffected by SIAs. The rest is only slightly affected. Moreover, the maximum concentration of SIAs is outside of the plastic zone. Open volume defects might have had some influence on an embrittlement of steel, but for sure they are not a major reason on embrittlement by the self-ion irradiation. Reason of hardening of this steel is rather on a precipitation and segregation of Cu (together with Ni) [38]. The Fe^{2+} ion irradiation is a sufficient tool to simulate neutron irradiation, mainly for its capability to make strong cascade collisions. These strong cascade collisions make a huge amount of primary knocked atoms and much more secondary knocked atoms, which are responsible for making of Frenkel defects and matrix damage, and also for an accelerating of precipitation of atoms; such are Cu, Ni or P.

6.11 Comparison of Vickers and nanohardness of JRQ steel - comparison of neutron and Fe^{2+} ion irradiation

For a better understanding of irradiation processes, a comparison with neutron irradiated specimens of JRQ steel was done. From a study made by Ulbricht [10, 11] at HZDR, here can be extracted Vickers hardness of irradiated JRQ steel in three fluencies (10, 77 and 139 x 10^{18} cm^{-2} (E > 0.5 MeV)) or exposures (0.010, 0.079 and 0.142 dpa), respectively, and convert Vickers hardness to nanoindentation hardness in order to compare them. Dpa values of neutron irradiated JRQ are based on Norgett-Robinson-Torrens (NRT) model for the dpa calculation according to [39]. NRT method for dpa calculation was proposed in order to bring a simple method for calculating the number of atoms displaced in a solid (especially in RPVs) during irradiation. It is assumed equivalence between NRT-dpa values for neutron irradiation and SRIM-dpa values for ion irradiation. This approximation could be done because current NRT-dpa standard is fully valid in the sense of a scaled radiation exposure measure, as it is essentially proportional to the radiation energy deposited per volume. As such, it is highly recommended to be used in reporting neutron results to enable comparison between different nuclear reactor environments and ion irradiations, as it is written and recommended by NEA (Nuclear Energy Agency) in [40].

The conversion is based on the definition of Vickers and indentation hardness assuming an ideal intender. The following equation (1) was suggested by Rice and Stoller [41], who made experimental correlation of Vickers and nanoindentation also for A533B steel.

$$\Delta H_{Vickers}\,[GPa] = 0.937\,\Delta H_{Indentation}\,[GPa] \quad (1)$$

Reported HV10 values were converted into equivalent nanohardness values. Firstly, HV10 (in kp/mm^2) was converted to GPa by multiplication with 0.009807. Then HV10 in GPa was converted to H_{IN} in GPa by dividing by 0.937 according to (16). Afterwards, the ISE was removed by adding the difference between measured (nanohardness of Fe^{2+} ions irradiated) and converted H_{IN} (Vickers of neutron irradiated) for the unirradiated condition (0.57 GPa) and assuming that the same shift is applicable to the neutron irradiated conditions. It will be able to do that if it is assumed that the ISE and the irradiation effect are two independent effects. Calculated and converted values of nanohardness of the all irradiated specimens are listed in Tab. 6.2.

Tab. 6.2 – Vickers and nanoindentation hardness of neutron and Fe^{2+} irradiated JRQ

Fluence (dpa)	**Neutron irradiation** – Vickers hardness		**Fe^{2+} Ion irradiation** - nanoindentations
	HV10	converted to H_{IN} (GPa)	H_{IN} (GPa) for 200 nm ind. depth
Unirradiated	204 ± 4	2.71 ± 0.04	
0.01 (NRT)	262 ± 5	3.31 ± 0.05	
0.079 (NRT)	287 ± 5	3.57 ± 0.05	
0.142 (NRT)	307 ± 5	3.78 ± 0.05	
0.01 (SRIM)			2.95 ± 0.08
0.03 (SRIM)			3.35 ± 0.10
0.10 (SRIM)			3.53 ± 0.13
0.30 (SRIM)			4.09 ± 0.10
1.00 (SRIM)			4.62 ± 0.11

There will be seen the same behaviour as we have seen in Fig. 6.17, if behaviour of hardness as a function of exposure (Tab. 6.2 and Fig. 6.18) is compared. Neutron irradiated JRQ steel shows also a rapid nanohardness increase up to approximately 0.01 dpa and then a slower increase. Also, the dependence does not indicate saturation in the range of measurement. This behaviour is usual in steels with higher Cu content, as has been also calculated by Debarberis et al. [2], where a quite rapid increase at low exposures is followed by a slower increase of hardness at high exposures. The hardness of measurements, neutron irradiated and ion irradiated, increased approximately with the same trend. The individual values of the hardness increase of neutron-irradiated JRQ (after conversion into H_{IN}) are different from the values obtained for ion-irradiated JRQ, most prominently at 0.01 dpa. Indeed, an agreement was not expected because of the approximations (equivalence between NRT and SRIM dpa, conversion of Vickers hardness) and differences between ion and neutron irradiation such as flux. The shapes of the H_{IN} (Fig. 6.18) versus dpa curves for neutron and ion irradiated material are surprisingly similar. This strongly indicates that the hardening features in neutron and ion irradiated material are the same and their evolution is closely related.

For neutron irradiated JRQ, it was shown before by means of PALS (in section 10.3) and Small-Angle-Neutron-Scattering (SANS) [11] that open volume defects (vacancies and small vacancy clusters concretely of level around 2-4 vacancies) are available to enhance solute atom diffusion. This gives rise to irradiation-enhanced formation of Cu-rich clusters as confirmed by means of SANS for the same neutron-irradiated conditions of JRQ [10]. There was also assumed that the mechanism of the irradiation hardening can be explained with the interaction between the glide dislocations and the dispersed obstacles to the dislocation motion produced by the irradiation defects. The fine-dispersed radiation defects can be regarded as weak, penetrable obstacles [10].

It can be stated that both types of irradiation cause increasing of hardness by the same mechanism, since the slow-positron measurement showed that it is not due to open volume defects accumulation, it will be most likely due to Cu precipitation, as shown in [10, 11]. There was shown that there is a pronounced correlation between hardening and square root of volume fraction of Cu-rich clusters (investigated by SANS) in neutron irradiated JRQ. Based on the nanohardness comparison and their similarity between the curves shapes observed in the present study, there is an assumption that Cu-rich clusters are also formed and evolved in Fe^{2+} ion irradiated JRQ (which is not self-evident) and govern the ion-irradiation-induced hardness increase.

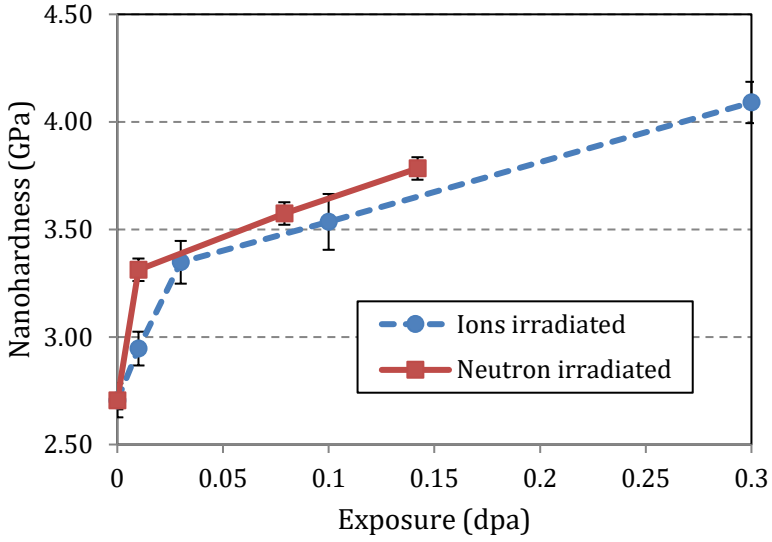

Fig. 6.18 - Comparison of neutron and Fe^{2+} ion irradiated JRQ specimens by dpa dependence of nanohardness (only values up to 0.3 dpa; lines do not indicate a model)

Another point of interest can be related to the change of slope. The volume fraction of Cu-rich clusters in JRQ neutron irradiated up to 0.01 dpa is 0.21 vol% [10]. This is more than what can be explained by the available Cu of 0.15 wt% (around 0.13 vol%). First, it can be concluded that other elements, most prominently Ni [38], contribute to the Cu-rich clusters. Second, it can be concluded that the rapid attachment of Cu atoms to the Cu-rich clusters is finished at approximately 0.01 dpa, because the availability of Cu from the matrix is exhausted. Afterwards other chemical elements such as Ni must be responsible for the further increase of the cluster volume fraction. This process proceeds at a lower rate. This reasoning shows that the exhaustion of available matrix Cu can also be the reason of the decrease of slope observed for ion-irradiated JRQ.

6.12 Analysis of JRQ steel

JRQ steel was the most comprehensively studied RPV steel in this thesis. The results based on slow-positron DBS, PALS and CDBS measurements of JRQ steel completed and confirmed suitability of PAS techniques for the vacancy type defects characterisation from intensity as well as volume of defects point of view. In contradiction to light ion implantation (He, H), the Fe^{2+} ion irradiation causes larger damage resulting in significant hardness changes and slow-positron DBS parameters. Therefore, Fe^{2+} ion irradiation seems to be the most recommended experimental simulation for relevant radiation damage studies without the specimen activation. The measured data from nanohardness and slow-positron DBS brings a new aspect to the wide topic under consideration of radiation embrittlement. Ion irradiation is a very useful tool, which saves time, money and reduces risk of unnecessary exposure of scientific workers. Nevertheless, there are still a lot of uncertainties and questions about accuracy and precision of ion irradiation in order to simulate a real radiation embrittlement, which occurs in nuclear reactors. Therefore, also experimental studies of slow-positron DBS and nanohardness were done in order to confront with our previous studies dedicated to the neutron irradiated steels.

It can be concluded that the following findings were found about Fe^{2+} ion irradiated JRQ steel:

1) The observed increasing trend of nanohardness caused by Fe^{2+} ion irradiation confirms that Cu precipitation is most likely responsible for the irradiation hardening. Atoms of Cu precipitate due to the irradiation, which brings a needed energy to this process in form of collisions of impacting particles.

2) The experimentally measured nanohardness is also in good agreement with Vickers hardness of the neutron irradiated JRQ samples after their conversion to nanohardness, which brings a finding that the hardening features in neutron and ion irradiated material are the same and their evolution is closely related.

3) Open volume (vacancy type) defects in the crystal lattice of JRQ steel were excluded from a responsibility for the hardness increase arising by the Fe^{2+} ion irradiation. Vacancy type defects were created immediately after the first level of the irradiation and then stayed at approximately same level. The vacancy-type defects themselves are too small to contribute significantly to the hardness increase. But they are responsible for irradiation-enhanced Cu diffusion, which gives rise to the formation of Cu-rich clusters and hardening.

4) Self-ion and neutron irradiations are different from a number of viewpoints including flux [42], injected interstitials for self-ion irradiations, thin damage layer for ions versus damaged bulk for neutrons and others. Irrespective of these differences, a surprising similarity of the hardness increase induced by ion and neutron irradiation was observed in the present case of the RPV steel JRQ containing 0.15 wt% of Cu. This result is encouraging for the application of ion irradiation to simulate neutron damage, even for such highly complex structures of RPV steels, particular in situations, where no or very little material is available.

5) There are still some peculiarities of ion irradiation in comparison with neutron irradiation. For instance, it was found out that open volume defects have different behaviour under neutron and Fe^{2+} ion irradiation. But it seems that hardening effect has most likely similar origin under both ways of irradiation.

6.13 Influence of Copper to evolution of radiation damage in RPV steels

The theory about Cu influence to hardening and embrittlement due to irradiation was explained before in Section 3.3.3., 3.5. and 3.6., respectively. Besides that, different experimental measurements support these theoretical based assumptions. The best agreement between model and different experimental data was found in JRQ steel, as was discussed in previous section. Another agreement can be found in Fig. 6.19, where neutron irradiated JRQ shows saturated behaviour by PALS after approximately 8.0×10^{19} cm^{-2} of fluence, what is in coincidence with slow-positron DBS measurement. Both results show that defects are not evolving or are saturated after some critical part of irradiation even in this steel with medium Cu content. Hardening or embrittlement in JRQ is not dependent on size and concentration of vacancy-type defects.

However, JPA steel with almost two times higher Cu content than JRQ (0.29 wt% in comparison with 0.15 wt%) showed a increase of τ_{avg} parameter (Fig. 6.19) during the whole neutron irradiation up to fluence of 14.3×10^{19} cm^{-2} and did not reach a saturation in the measured range. From this, it can be concluded that high Cu content may have an influence on the defect growth. Also, the rapid increase of τ_{avg} parameter was observed in JPA, which is presumed and supposed in steels with higher Cu content. Higher amount of Cu atoms is available to precipitate and also to serve as nucleation sites for the defect aggregates, because Cu causes the formation of many smaller defect aggregates during irradiation [43]. Moreover, German RPV steels shows similar behaviour, where P16WM,

modern steel with lower Cu content (0.08 wt%) has more homogenously dispersed smaller defects after the neutron irradiation than P370WM steel with higher Cu content (0.22 wt%).

German high-Cu steel P370WM was irradiated in MTR up to fluence of ~2.2x10^{19} cm^{-2}. Two cuts from the same irradiated bulk were measured by PALS and showed quite different results. τ_{avg} parameter increased by values of approximately 5 and 15 ps, respectively. There can be plotted (Fig. 6.20) an area, where can be estimated that the growth of τ_{avg} parameter should be in from measured data (blue dashed lines). But in the high-Cu steel can be assumed a steep increase followed by a slighter slope. Nevertheless, measured data for H^+ ion irradiated sample of P370WM steel show exactly this expected behaviour. H^+ ion irradiation was fortunately done in three fluencies, where it was able to obtain the steep increase after first fluence. After that, the increase is slight and in the range of neutron irradiated samples (in the area of blue dashed lines). The ability of H^+ ion irradiation to assist neutron irradiation was proven here, where more precise gradation is needed, and it is not available. These results support the assumption [2] of exponential increase of damage (interpreted by the defect concentration) during irradiation in high-Cu materials.

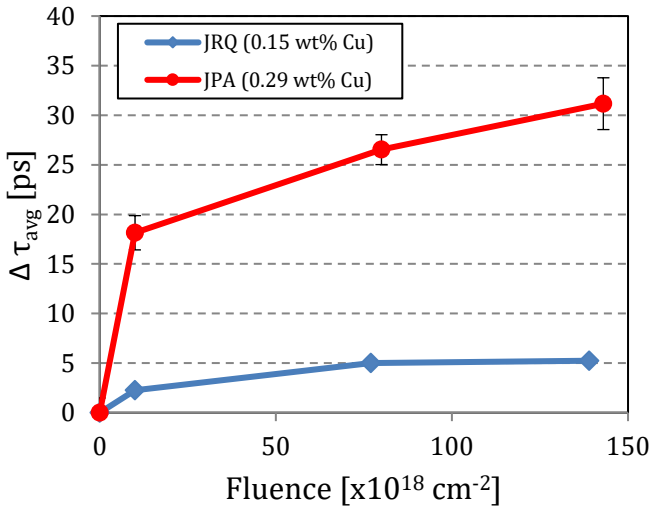

Fig. 6.19 - Average positron lifetime change of Japan model steels as a function of neutron fluence

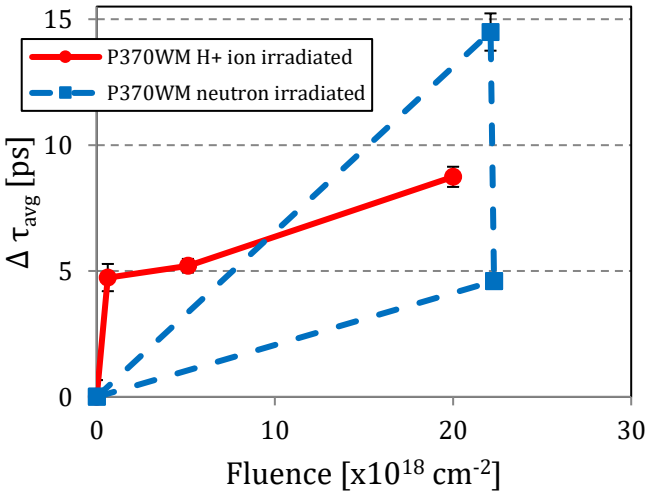

Fig. 6.20 - Average positron lifetime change as a function of neutron fluence for P370WM steel

7 MAIN FINDINGS AND BENEFITS

- Unique PALS and CDBS measurements were done with different western neutron irradiated RPV steels, which have partially contributed to the overall understanding of neutron irradiation effect by means of the open volume defects creation. These results were used also in different international projects dedicated to RPV embrittlement study and other material issues and were internationally recognised and published in several peer reviewed journals.

- The comprehensive database was created with experimental data of neutron and ion irradiated (H^+ and Fe^{2+}) RPV steels, especially of JRQ steel, with different irradiation conditions such as fluencies or thermal annealing. These different approaches of irradiation were examined and evaluated in order to confirm possibilities to simulate neutron irradiation experimentally by ion implantation. Both ways of ion irradiation, H^+ and F^{2+}, were able to support, complement or even predict future trends of neutron irradiated RPV steels samples by means of PALS, slow-positron DBS and nanohardness measurements.

- PALS studies were accompanied with other different experimental techniques like CDBS, slow-positron DBS and nanoindentation, at INPE and HZDR as well. The comparison was done with other experimental techniques, especially with Vickers hardness and SANS, which were performed

at HZDR, too. Moreover, PALS results were supported and complemented by means of cluster dynamics simulations reported in [44, 45].

- It has been confirmed that Cu precipitation is most likely responsible for the irradiation hardening by both types of irradiation; neutron and Fe^{+2} ion irradiation. The hardening features are the same in neutron and Fe^{2+} ion irradiated materials and their evolution is closely related, which was observed in JRQ steel with medium Cu content (0.15 wt%).

- Slow-positron DBS have confirmed that open volume defects are not responsible for the hardness increasing by Fe^{+2} ion irradiation in JRQ steel. These defects were created during the first step of irradiation and then remained at approximately same level or increased very slowly with the fluence increasing. Nevertheless, they are responsible for irradiation-enhanced Cu diffusion, formation of Cu-rich clusters, which are responsible for hardening and embrittlement of RPVs.

- There was observed the steep increase of the average positron lifetime in the steel with the highest Cu content investigated in this thesis – JPA (0.29 wt%). A similar finding was identified also in P370WM (0.22 wt% of Cu) steel irradiated by H^+ ions, where the irradiation caused the same rapid increase of the average positron lifetime. There was no complete saturation in the measured fluence range in both steels. Higher Cu content is most likely responsible for ongoing defects creation during irradiation compared to JRQ steel with medium Cu content, where defects concentration is almost saturated after initial levels of irradiation.

- It was observed via PALS that relatively low Cu content of P16WM steel (0.08 wt%) does not guarantee also the lowest average positron lifetime, if there was a quite large amount of Ni in the content (1.69 wt%).

- The thermal annealing experiment of JRQ confirmed the effectiveness of this procedure by means of PALS and CDBS. There was found different ideal annealing temperatures about 425 °C for CDBS and 475 °C for PALS.

- Last but not least, ion irradiation is a common practise for characterisation of new materials such as ferritic/martensitic Chromium steels or ODS steels, but such kinds of studies are rare for RPV steels. Benefits of ions to simulate neutron damage, in such complicated and complex materials as RPV steels, is still under discussion. Hopefully, this thesis could bring new experimentally supported piece of knowledge in this area.

8 CONCLUSION

This thesis is focused on the problem of radiation damage in RPV steels in terms of safe and feasible long-term operation of NPPs. Radiation damage mostly in the form of neutrons is responsible for a constant change of the whole set of nuclear-physical properties of materials. All of this negatively affects a size of open volume defects, precipitation and segregation of solute atoms influencing hardening and embrittlement, radioactive isotopes cumulating in the material. Moreover, grain boundaries are distorted by helium and hydrogen molecules. These microscopic effects result to macroscopic ones, such as DBTT shift and gradual creation of cracks. Since RPV is not reasonably replaceable and reparable, a special care must be taken to secure the best possible condition of RPV during the operation.

As an essential part of this thesis, four types of neutron irradiated western RPV steels were investigated by different non-destructive PAS techniques. Studied RPV steels were differed mainly from chemical composition point of view, especially from Cu and Ni contents. The material characterization was done via positron based experimental techniques from defects size and defects concentration standpoints. All of this was executed in order to investigate and characterize the microstructure evolution of the different neutron irradiated RPV steels.

Experimental analyses focused on PALS showed that steels in the unirradiated state contain relatively small amounts of defects on level of monovacancies-divacancies. There were observed different types of behaviour after the neutron irradiation. One type was increasing of defect size and another was increasing of intensity of annihilations in defects. That means that the neutron irradiation caused the defect growth via clustering or the increase of the number of defects.

Besides determining the damage level in materials, it is important to know an accurate trend of material degradation. For this task, radiation damage has been experimentally simulated using additional ion irradiation by light and heavy ions and compared to neutron irradiated RPV samples. JRQ steel was irradiated by Fe^{2+} ions and P370WM was irradiated by H^{+} ions. In the case of German P370WM, the same fluence was reached as was in the neutron irradiated sample. As a result, there was able to observe the studied phenomenon of rapid average positron lifetime increase after the first level of irradiation. The same increasing trend was observed in JRQ steel after ion and neutron irradiation as well. Steels with highest Cu content have had this trend relatively higher. Copper responsibility for this, by immediate precipitation after the irradiation, was most likely proved with nanohardness measurement and its comparison with Vickers hardness.

It was observed that the effects responsible for Fe^{2+} ion irradiation hardening has most likely common the same features with neutron irradiation induced hardening or their evolution is closely related, especially in medium-Cu RPV steel. Thus, there was proven the ability to simulate neutron irradiation by ion irradiation in order to investigate the hardening effect of RPV steels. It is recommended to use heavy ions accompanied with light ions with regard to get more complex irradiated spectrum, which is more comparable to the neutron damage spectrum.

The benefits of this work are related mainly to a uniqueness of measuring and comparing neutron and ions irradiated RPV steels by PAS techniques. Additionally, even though ion irradiation to RPV steels is still under discussion, it was proven in this thesis that the simulation of neutron irradiation by ions can be beneficial also to RPV steels. The best use of ion irradiation can be as supplement data, where only small amount of reference material is available. In terms of extension of NPPs lifetime, a lot of surveillance programs will be touched (limited) with small amount of an unirradiated reference material. A lack of virgin material can cause a variety of difficulties and it can be harder to predict a longer operation than it was designed. This is the area, where ion irradiation can find its application.

9 REFERENCES

[1] SLUGEŇ, V.: Safety of VVER-440 Reactors – Barriers Against Fission Products Release. Springer, 2011. ISBN 978-1-84996-419-7.

[2] DEBARBERIS, L. et al.: Int. J. Pres. Ves. Pip., vol. 82, 2005.

[3] NOMOTO, A.: Understanding on the Mechanisms of Irradiation Embrittlement of RPV Steels and Development of Embrittlement Correlation Method. CRIEPI, IAEA. In: Training Workshop on Assessment of Degradation Mechanisms of Primary Components in Water Cooled Nuclear Reactors: Current Issues and Future Challenges, CIEMAT – Madrid, 2014.

[4] NANSTAD, R.: Review of Progress and Major Challenges for Ensuring the Performance of PWR Pressure Vessels for Long Time Service. In: International Workshop on RPV Embrittlement and Surveillance Programmes, Czech Republic – Prague, 2015.

[5] WAS, G. S.: Fundamentals of Radiation Materials Science: Metals and Alloys. Springer, 2007. ISBN 978-3-540-49471-3.

[6] HEIN, H. et al.: Journal of ASTM International, vol. 6(7), 2009, Paper ID: JAI101962.

[7] HEIN, H. et al.: PVP2009-77035. In: Proceeding of the ASME 2009 Pressure Vessels and Piping Division Conference, Prague, 2009.

[8] IAEA NUCLEAR ENERGY SERIES NO. NP-T-3.11.: Integrity of Reactor Pressure Vessel in Nuclear power Plants: Assessment of Irradiation Embrittlement Effects in Reactor Pressure Vessel Steels. 2009. URL: http://www-pub.iaea.org/MTCD/ Publications/ PDF/Pub1382_web.pdf.

[9] STEELE, L. E.: Radiation Embrittlement of Nuclear Reactor Pressure Vessel Steels, An International Review – 4th Volume. In: ASTM International, 1993. ISBN 0803114788.
[10] ULBRICHT, A. et al.: Journal of ASTM International, vol. 2(10), 2005, Paper ID: JAI12385.
[11] ULBRICHT, A. et al.: J. Nucl. Mater., vol. 353, 2006, pp. 27-34.
[12] SABELOVÁ, V.: Study of the radiation resistance of alloys based on Fe-Cr. Doctoral thesis, INPE FEI STU, 2014.
[13] ANWAND, W. et al.: Appl. Surf. Sci., vol. 194, 2002, pp. 131-135.
[14] BUTTERLING, M.: Application of High-Energy Photons for Positron Annihilation Spectroscopy and Positronium Chemistry. Doctoral thesis, Martin Luther University Halle-Wittenberg, 2014. URL: http://d-nb.info/1054950660/34.
[15] HEINTZE, C. et al.: J. Nucl. Mater., vol. 472, 2016, pp. 196-205.
[16] HAUTOJÄRVI, P. et al.: J. Nucl. Mater., vol. 114, 1983, pp. 250.
[17] VEHANEN, A. et al.: Phys. Rev. B, vol. 25, 1982, pp. 762.
[18] BRAUER, G. et al.: Report ZfK 647, 1990.
[19] SAITO, H. et al.: Nucl. Instrum. Meth. A, vol. 487, 2002, pp. 612-617.
[20] SLUGEŇ, V.: What Kind of Information We Can Obtain from Positron Annihilation Spectroscopy. In: DG JRC Institute for Energy, 2006.
[21] NUGENIA ASSOCIATION: RPV Irradiation Embrittlement. In: NUGENIA position on RPV Irradiation Embrittlement issues on the outcome of the EURATOM FP7 project LONGLIFE, 2014.
[22] SLUGEŇ, V. et al.: J. Nucl. Mater., vol. 274, 1999, pp. 273-286.
[23] BOYDON, F. M. D. et al.: Low Temperature Embrittlement of RPV Support Structure Steel. In: Effects of Radiation on Materials: 17th International Symposium ASTM STP 1270, 1996.
[24] SONEDA, N.: Irradiation Embrittlement of Reactor Pressure Vessels (RPVs) in Nuclear Power Plants. Elsevier, 2014. ISBN 0857096478.
[25] BALLESTEROS, A.: Annealing and Re-Embrittlement of Reactor Pressure Vessel Materials. JRC European Commission, In: PRIMAVERA Seminar – Petten, 2011.
[26] KRYUKOV, A. et al.: J. Nucl. Mater. vol. 429, 2012, pp. 190–200.
[27] REPKA, M.: Management of the Bohunice RPVs Annealing Procedure. In: International Workshop on WWER-440 Reactor Pressure Vessel Embrittlement and Annealing, Závažná Poruba, Slovak Republic, 1994.
[28] IAEA-TECDOC-1435: Application of surveillance programme results to reactor pressure vessel integrity assessment, April (2005), URL: http://www-pub.iaea.org/ MTCD/Publications/PDF/te_1435_web.pdf.
[29] SERVER, W.: Mitigative Options including Thermal Annealing to Extend RPV Life and Recover Properties. ATI Consulting, In: IAEA Training Workshop on Assessment of Degradation Mechanisms of Primary Components in Water Cooled Nuclear Reactors: Current Issues and Future Challenges, CIEMAT – Madrid, 2014.
[30] SLUGEŇ, V. et al.: NDT&E International, vol. 37, 2004, pp. 651-661.
[31] DOERNER, M. F., NIX, W. D.: J. Mater. Res., vol. 601, 1986.
[32] OLIVER, W. C., PHARR, G. M.: J. Mater. Res., vol. 7, 1992, pp. 1564–1583. ISSN 2044-5326.
[33] OLIVER, W. C., PHARR, G. M.: J. Mater. Res., vol. 19, 2004, pp. 3.
[34] HEINTZE, C. et al.: J. Nucl. Mater., vol. 417, 2011, pp. 980-983.
[35] NIX, W.D., GAO, H.: J. Mech. Phys. Solids, vol. 46, 1998, pp. 411–425.
[36] HARDIE, C. D., ROBERTS, S. G.: J. Nucl. Mater., vol. 433, 2013, pp. 174-179.
[37] FISCHER-CRIPPS, A. C.: Surf. Coat. Tech., vol. 200, 2006, pp. 4153-4165.
[38] BUSWELL. J. T. et al.: Nucl. Mater., vol. 225, 1995, pp. 196-214.
[39] NORGETT, M. J. et al.: Nuc. Eng. Des., vol. 33, 1975, pp. 50-54.
[40] NEA-OECD: Primary Radiation Damage in Materials. OECD, 2015. URL: https://www.oecd-nea.org/science/docs/2015/nsc-doc2015-9.pdf.
[41] RICE, P.M., STOLLER, R.E.: MRS Proceedings, vol. 649, 2011).
[42] BERGNER, F. et al.: J. Phys. Condens. Matter, vol. 20, 2008, pp. 104262.
[43] SMIDT, F. A. Jr., SPRAGUE, J. A.: Effects of Radiation on Substructure and Mechanical Properties of Metals and Alloys. STP 529, American Society for Testing and Materials, Philadelphia, 1973, pp. 78-91.
[44] SLUGEŇ, V. et al.: Radiat. Eff. Defect S., vol. 171, 2016, pp. 231-241.
[45] GOKHMAN, A. et al.: Radiat. Eff. Defect S., vol. 170, No. 9, 2015, pp. 745-757.

10 LIST OF PUBLICATIONS

Scientific articles in peer reviewed (CC) journals:

[1] GOKHMAN, Aleksandr - PECKO, Stanislav - SLUGEŇ, Vladimír. Cluster dynamics study of damage accumulation in helium-implanted Fe–2.5at%Cr alloy. In *Radiation Effects and Defects in Solids*. Vol. 170, No. 2 (2015), pp. 130-137. ISSN 1042-0150.

[2] GOKHMAN, Aleksandr - PECKO, Stanislav - SLUGEŇ, Vladimír. Simulation of *nanostructure* evolution under helium implantation in Fe–(2.5–12.5)at% Cr alloys at a temperature of 343 K. In *Radiation Effects and Defects in Solids*. Vol. 170, No. 9 (2015), pp. 745-757. ISSN 1042-0150.

[3] PECKO, Stanislav - SOJAK, Stanislav - SLUGEŇ, Vladimír. Comparative study of irradiated and hydrogen implantation damaged German RPV steels from PAS point of view. In *Applied Surface Science*. Vol. 312 (2014), pp. 172-175. ISSN 0169-4332.

[4] PECKO, Stanislav - SOJAK, Stanislav - SLUGEŇ, Vladimír. Comparison of irradiated and hydrogen implanted German RPV steels using PAS technique. In *Nuclear Instruments & Methods in Physics Research Section B - Beam Interactions with Materials and Atoms*. Vol. 365, Part. A, (2015), pp. 222–224. ISSN 0168-583X.

[5] PECKO, Stanislav - PETRISKA, Martin - SOJAK, Stanislav - SLUGEŇ, Vladimír. Positron *annihilation* lifetime study of JRQ and JPA irradiated and annealed reactor pressure vessel steels. In *Progress in Nuclear Energy*. Vol. 87, (2016), pp. 15-19. ISSN 0149-1970.

[6] PECKO, Stanislav - HEINTZE, Cornelia - BERGNER, Frank - ANWAND, Wolfgang - SLUGEŇ, Vladimír. Fe^{2+} ion irradiated JRQ steel investigated by nanoindentation and slow-positron Doppler broadening spectroscopy. In *Nuclear Instruments & Methods in Physics Research Section B - Beam Interactions with Materials and Atoms*. Vol. 415, (2018), pp. 1–8. ISSN 0168-583X.

[7] RÖDER, Falk - HEINTZE, Cornelia - PECKO, Stanislav - AKHMADALIEV, S. - BERGNER, Frank - ULBRICHT, Andreas - ALTSTADT, Eberhard. Nanoindentation of ion-irradiated reactor pressure vessel steels – model-based interpretation and comparison with neutron irradiation. In *Philosophical Magazine, Structure and Properties of Condensed Matter*. Vol. 98:11, (2018), pp. 911–933. ISSN 1478-6435.

[8] SLUGEŇ, Vladimír - HEIN, H. - SOJAK, Stanislav - PECKO, Stanislav - VETERNÍKOVÁ, Jana - PETRISKA, Martin - SABELOVÁ, Veronika - BARTOŠOVÁ, Iveta - STACHO, Matúš. German and Russian irradiated reactor pressure vessel steels from PAS point of view. In *Acta Physica Polonica A: Proceedings of the 41st Polish Seminar on Positron Annihilation, Lublin, 9-13 Sept. 2013*. pp. 726-728. ISSN 0587-4246.

[9] SLUGEŇ, Vladimír - PECKO, Stanislav - SOJAK, Stanislav. Experimental studies of irradiated and *hydrogen* implantation damaged reactor steels. In *Journal of Nuclear Materials*. Vol. 468, (2016), pp. 285-288. ISSN 0022-3115.

[10] SLUGEŇ, Vladimír - GOKHMAN, Aleksandr - PECKO, Stanislav - SOJAK, Stanislav – BERGNER, Frank. JRQ and JPA irradiated and annealed reactor pressure vessel steels studied by positron annihilation. In *Radiation Effects and Defects in Solids*. Vol. 171, No. 3-4 (2016), pp. 231-241. ISSN 1042-0150.

Scientific articles at domestic journals registered in Web of Science or SCOPUS:

[11] NOVÁK, Patrik - GOKHMAN, Aleksandr - DOBROČKA, Edmund - BOKOR, Jozef - PECKO, Stanislav. Investigation of helium implanted Fe-Cr alloys by means of x-ray diffraction and positron annihilation spectroscopy. In *Journal of Electrical Engineering*. Vol. 66, No. 6 (2015), pp. 334–338. ISSN 1335-3632.